REPORT DOCUMENTATION PAGE

Form Approved
OMB No. 0704-0188

1. REPORT DATE *(DD-MM-YYYY)*	2. REPORT TYPE	3. DATES COVERED *(From - To)*
25/Jun/2001	MAJOR REPORT	

4. TITLE AND SUBTITLE
BOLT LOAD RETENTION BEHAVIOR OF A DIE CAST MAGNESIUM RARE EARTH ALLOY

5a. CONTRACT NUMBER

5b. GRANT NUMBER

5c. PROGRAM ELEMENT NUMBER

6. AUTHOR(S)
CAPT MORENO IAN P

5d. PROJECT NUMBER

5e. TASK NUMBER

5f. WORK UNIT NUMBER

7. PERFORMING ORGANIZATION NAME(S) AND ADDRESS(ES)
UNIVERSITY OF MICHIGAN

8. PERFORMING ORGANIZATION REPORT NUMBER
CI01-123

9. SPONSORING/MONITORING AGENCY NAME(S) AND ADDRESS(ES)
THE DEPARTMENT OF THE AIR FORCE
AFIT/CIA, BLDG 125
2950 P STREET
WPAFB OH 45433

10. SPONSOR/MONITOR'S ACRONYM(S)

11. SPONSOR/MONITOR'S REPORT NUMBER(S)

12. DISTRIBUTION/AVAILABILITY STATEMENT
Unlimited distribution
In Accordance With AFI 35-205/AFIT Sup 1

13. SUPPLEMENTARY NOTES

14. ABSTRACT

20010720 021

15. SUBJECT TERMS

16. SECURITY CLASSIFICATION OF:			17. LIMITATION OF ABSTRACT	18. NUMBER OF PAGES	19a. NAME OF RESPONSIBLE PERSON
a. REPORT	b. ABSTRACT	c. THIS PAGE			19b. TELEPHONE NUMBER *(Include area code)*

Ian P. Moreno
Captain, USAF
2001

Master of Science in Engineering (M.S.E.) in Materials Science and Engineering
University of Michigan, Ann Arbor

The following abstracts are taken from the papers Captain Moreno wrote describing his research while a master's student at the U of M. This work, along with the completion of required courses and presentations at major research conferences, fulfilled the requirements imposed by his advisors, his department, and the Horace H. Rackham School of Graduate Studies for the awarding of his M.S.E. degree. The following describes the publishing status of these papers.

Bolt-Load Retention Behavior of a Die Cast Magnesium-Rare Earth Alloy

- Published in March 2001 by the Society of Automotive Engineers, SAE Technical Paper Series, Paper 2001-01-0425

Microstructural Characterization of a Die Cast Magnesium-Rare Earth Alloy

- To be submitted for publishing, June 2001, in the journal: *Scripta* Materialia

Creep Behavior of a Die Cast Magnesium-Rare Earth Alloy

- To be submitted for publishing, July 2001, in the journal: Metallurgical and Materials Transactions A

Bolt-Load Retention Behavior of a Die Cast Magnesium-Rare Earth Alloy

Ian P. Moreno, Keun Yong Sohn*, and J. Wayne Jones
Materials Science and Engineering Department, University of Michigan

John E. Allison
Materials Science Department, Ford Research Laboratory, Ford Motor Co.

*Now with Korea Institute of
Machinery and Materials (KIMM)

The need for improved understanding of new magnesium alloys for the automotive industry continues to grow as the application for these lightweight alloys expands to more demanding environments, particularly in drivetrain components. Their use at elevated temperatures, such as in transmission cases, presents a challenge because magnesium alloys generally have lower creep resistance than aluminum alloys currently employed for such applications. In this study, a new die cast magnesium alloy, MEZ, containing rare earth (RE) elements and zinc as principal alloying constituents, was examined for its bolt-load retention (BLR) properties. Preloads varied from 14 to 28 kN and test temperatures ranged from 125 to 175°C. At all test temperatures and preloads, MEZ retained the greatest fraction of the initial imposed preload when compared to the magnesium alloys AZ91D, AE42, AM50, and the AM50+Ca series alloys. The BLR behavior of MEZ did not show significant sensitivity to temperature within the range examined, whereas the other alloys displayed a clear decrease in bolt-load retention with increased temperature at a given preload. Retained bolt-load decreased for MEZ with increasing preload in a manner similar to the behavior of other alloys. The higher BLR can be attributed to the greater resistance to creep and arises mainly from the Mg-RE phases present at cell and grain boundaries and the relatively high solidus temperature (T_s) of MEZ. Additional means of improving BLR by varying geometrical dimensions in the bolted assembly for AZ91D and AM50 were investigated and no significant improvement was observed in the limited studies that were performed.

Microstructural Characterization Of A Die Cast Magnesium-Rare Earth Alloy

I.P. Moreno[1], T.K. Nandy[1], J.W. Jones[1], J.E. Allison[2], and T.M. Pollock[1]
[1]University of Michigan, Materials Science and Engineering, Ann Arbor, MI 48109, USA
[2]Materials Science Department, Ford Motor Co., Dearborn, MI 48126, USA

Keywords: Magnesium; Die Casting; Scanning/transmission electron microscopy (STEM); Electron diffraction; Electron microprobe analysis

Microstructural characterization of high-pressure die cast alloy MEZ (Mg-2.5RE-0.35Zn-0.3Mn) reveals equiaxed cells of α-Mg with a partially divorced interdendritic eutectic. Detailed diffraction studies coupled with WDS analysis shows the presence of a continuous $Mg_{12}RE$ intermetallic phase in the eutectic aggregate along with fine MgO particles.

Creep Behavior of a Die Cast Magnesium-Rare Earth Alloy

I.P. MORENO, J.W. JONES, and J.E. ALLISON

The tensile and compressive creep behavior of experimental HPDC alloy, MEZ, shows significant improvement over benchmark alloy AE42 and other magnesium alloys under development for high temperature automotive applications. Improved high temperature creep resistance is attributed to a stable, continuous $Mg_{12}RE$ intermetallic phase much different in morphology than the intergranular phase found in AE42 and other Mg-Al alloys. The role of microstructure on the short and long term mechanical response is heavily influenced by the presence of aluminum in Mg alloys, and the superior creep performance of this alloy is largely attributed to its absence. Tensile and compressive creep behavior is uniform and correlates with the bolt-load retention behavior of this alloy. Thermal and mechanical properties are related to the different stages of creep in MEZ.

Ian P. Moreno
Captain, USAF
2001

Master of Science in Engineering (M.S.E.) in Materials Science and Engineering
University of Michigan, Ann Arbor

The following abstracts are taken from the papers Captain Moreno wrote describing his research while a master's student at the U of M. This work, along with the completion of required courses and presentations at major research conferences, fulfilled the requirements imposed by his advisors, his department, and the Horace H. Rackham School of Graduate Studies for the awarding of his M.S.E. degree. The following describes the publishing status of these papers.

Bolt-Load Retention Behavior of a Die Cast Magnesium-Rare Earth Alloy

- Published in March 2001 by the Society of Automotive Engineers, SAE Technical Paper Series, Paper 2001-01-0425

Microstructural Characterization of a Die Cast Magnesium-Rare Earth Alloy

- To be submitted for publishing, June 2001, in the journal: *Scripta* Materialia

Creep Behavior of a Die Cast Magnesium-Rare Earth Alloy

- To be submitted for publishing, July 2001, in the journal: Metallurgical and Materials Transactions A

Bolt-Load Retention Behavior of a Die Cast Magnesium-Rare Earth Alloy

Ian P. Moreno, Keun Yong Sohn*, and J. Wayne Jones
Materials Science and Engineering Department, University of Michigan

John E. Allison
Materials Science Department, Ford Research Laboratory, Ford Motor Co.

*Now with Korea Institute of
Machinery and Materials (KIMM)

The need for improved understanding of new magnesium alloys for the automotive industry continues to grow as the application for these lightweight alloys expands to more demanding environments, particularly in drivetrain components. Their use at elevated temperatures, such as in transmission cases, presents a challenge because magnesium alloys generally have lower creep resistance than aluminum alloys currently employed for such applications. In this study, a new die cast magnesium alloy, MEZ, containing rare earth (RE) elements and zinc as principal alloying constituents, was examined for its bolt-load retention (BLR) properties. Preloads varied from 14 to 28 kN and test temperatures ranged from 125 to 175°C. At all test temperatures and preloads, MEZ retained the greatest fraction of the initial imposed preload when compared to the magnesium alloys AZ91D, AE42, AM50, and the AM50+Ca series alloys. The BLR behavior of MEZ did not show significant sensitivity to temperature within the range examined, whereas the other alloys displayed a clear decrease in bolt-load retention with increased temperature at a given preload. Retained bolt-load decreased for MEZ with increasing preload in a manner similar to the behavior of other alloys. The higher BLR can be attributed to the greater resistance to creep and arises mainly from the Mg-RE phases present at cell and grain boundaries and the relatively high solidus temperature (T_s) of MEZ. Additional means of improving BLR by varying geometrical dimensions in the bolted assembly for AZ91D and AM50 were investigated and no significant improvement was observed in the limited studies that were performed.

Microstructural Characterization Of A Die Cast Magnesium-Rare Earth Alloy

I.P. Moreno[1], T.K. Nandy[1], J.W. Jones[1], J.E. Allison[2], and T.M. Pollock[1]
[1]University of Michigan, Materials Science and Engineering, Ann Arbor, MI 48109, USA
[2]Materials Science Department, Ford Motor Co., Dearborn, MI 48126, USA

Keywords: Magnesium; Die Casting; Scanning/transmission electron microscopy (STEM); Electron diffraction; Electron microprobe analysis

Microstructural characterization of high-pressure die cast alloy MEZ (Mg-2.5RE-0.35Zn-0.3Mn) reveals equiaxed cells of α-Mg with a partially divorced interdendritic eutectic. Detailed diffraction studies coupled with WDS analysis shows the presence of a continuous $Mg_{12}RE$ intermetallic phase in the eutectic aggregate along with fine MgO particles.

Creep Behavior of a Die Cast Magnesium-Rare Earth Alloy

I.P. MORENO, J.W. JONES, and J.E. ALLISON

The tensile and compressive creep behavior of experimental HPDC alloy, MEZ, shows significant improvement over benchmark alloy AE42 and other magnesium alloys under development for high temperature automotive applications. Improved high temperature creep resistance is attributed to a stable, continuous $Mg_{12}RE$ intermetallic phase much different in morphology than the intergranular phase found in AE42 and other Mg-Al alloys. The role of microstructure on the short and long term mechanical response is heavily influenced by the presence of aluminum in Mg alloys, and the superior creep performance of this alloy is largely attributed to its absence. Tensile and compressive creep behavior is uniform and correlates with the bolt-load retention behavior of this alloy. Thermal and mechanical properties are related to the different stages of creep in MEZ.

2001-01-0425

Bolt-Load Retention Behavior of a Die Cast Magnesium-Rare Earth Alloy

Ian P. Moreno, Keun Yong Sohn*, and J. Wayne Jones
Materials Science and Engineering Department, University of Michigan

John E. Allison
Materials Science Department, Ford Research Laboratory, Ford Motor Co.

*Now with Korea Institute of
Machinery and Materials (KIMM)

ABSTRACT

The need for improved understanding of new magnesium alloys for the automotive industry continues to grow as the application for these lightweight alloys expands to more demanding environments, particularly in drivetrain components. Their use at elevated temperatures, such as in transmission cases, presents a challenge because magnesium alloys generally have lower creep resistance than aluminum alloys currently employed for such applications. In this study, a new die cast magnesium alloy, MEZ, containing rare earth (RE) elements and zinc as principal alloying constituents, was examined for its bolt-load retention (BLR) properties. Preloads varied from 14 to 28 kN and test temperatures ranged from 125 to 175°C. At all test temperatures and preloads, MEZ retained the greatest fraction of the initial imposed preload when compared to the magnesium alloys AZ91D, AE42, AM50, and the AM50+Ca series alloys. The BLR behavior of MEZ did not show significant sensitivity to temperature within the range examined, whereas the other alloys displayed a clear decrease in bolt-load retention with increased temperature at a given preload. Retained bolt-load decreased for MEZ with increasing preload in a manner similar to the behavior of other alloys. The higher BLR can be attributed to the greater resistance to creep and arises mainly from the Mg-RE phases present at cell and grain boundaries and the relatively high solidus temperature (T_s) of MEZ. Additional means of improving BLR by varying geometrical dimensions in the bolted assembly for AZ91D and AM50 were investigated and no significant improvement was observed in the limited studies that were performed.

INTRODUCTION

Weight reduction remains an important goal in the automotive industry and the replacement of current materials with magnesium die cast alloys that can meet the targeted properties offers significant potential. The conventional high volume production magnesium alloys, such as high pressure die cast (HPDC) AZ91D and AM50, are limited to operating temperatures well below 150°C because of their poor elevated temperature creep properties. These alloys cannot be utilized in powertrain components such as automatic transmission cases where typical operating conditions can exceed this temperature.

Among the several magnesium alloys identified as potential replacements for aluminum-based alloys used in elevated temperature components, AE42 has been shown to be the most promising because of its superior creep resistance compared to AZ91D [1,2,3,4]. Although the cost of producing rare earth-containing alloys is a limiting factor and is reflected in their restricted use, it has been determined that the operating costs for casting and trimming AE42 would be similar to that of AZ91D if manufactured in comparable volumes [3]. The elevated temperature creep strength of AE42 has been attributed to rare earth additions that increase the volume fraction of higher melting, stable Al-RE phases [4,5]. AE42 offers creep resistance superior to other Mg-Al alloys but still displays marginal performance at 175°C [6]. It has been stated or inferred by some [1,7,8] that substantial improvement in creep resistance may come only with the development of a magnesium alloy outside of the Mg-Al system.

Magnesium Elektron, Inc. (Newcastle, UK) has developed a new alloy, designated Elektron MEZ, and

has reported creep results superior to other Mg alloys considered for high temperature automotive applications, including AE42 [1,9]. Die castability was demonstrated in the production of a filter housing, gearbox, and oil pan. Corrosion resistance was similar to that of high purity Mg alloys. This paper reviews the bolt-load retention behavior of MEZ and material properties that contribute to its resistance to creep.

As an alternative to investing in more costly alloy systems, design changes in fastener configuration may hold promise where BLR is critical. For example, Pettersen and Fairchild reported substantial improvement in the bolt-load retention of AZ91D by varying the thickness and diameter of washers in their test assembly [10]. In the present study similar tests were conducted on AZ91D and AM50 using different fastener configurations. The results are described in this paper.

EXPERIMENTAL PROCEDURE

MEZ, with a nominal composition of Mg-2.5%RE-0.35%Zn-0.3%Mn, was pressure die cast at Mag-tec Casting Corporation (Jackson, MI) in a four-cavity die. Components used in the BLR test configuration, cylindrical tensile/creep and fatigue blanks were produced. Melt and die temperatures were 700-710°C and 177-232°C, respectively. Gate velocities were 32.9, 30.5, 28.3, and 28.3 m/s for case, flange, tensile/creep, and fatigue samples, respectively. The actual composition of as-cast MEZ obtained by inductively coupled plasma (ICP)-atomic emission spectroscopy and mass spectrometer on a bulk flange specimen, is given in Table 1, along with compositions of materials from other studies [4,11].

Cast components of the bolt-load retention assembly consisted of a flange and case as shown in Figure 1. The flange and case have a 40x40mm contact surface with a centered 11mm diameter hole. The wall of the threaded case hole is 4mm thick and is supported by four 4mm thick ribs. The BLR assembly is shown in Figure 2, where a standard M10 bolt, machined just below the head to accommodate a bonded four-strain gage assembly in a 90° T rosette layout, passes through the flange and is threaded into the tapped BLR case. The assembly, simulating the actual fastener and boss geometry in a typical automatic transmission housing, was machined to a 1.6μm finish on the mating surfaces.

Transmission bolts are commonly torqued to preloads of 75-90% of the bolt proof strength. Specimens were torqued slightly above a nominal preload level of 14, 21, or 28kN at room temperature and held for approximately one hour before being submersed in a silicon oil bath held constant to within ±0.1°C of 125, 150, and 175°C. This waiting period minimizes the effects of short-term relaxation following tightening of bolted joints, as described in [12]. Tests were conducted at least 100 hours, and data was amplified and scaled using the Measurements Group System 2210 signal conditioner

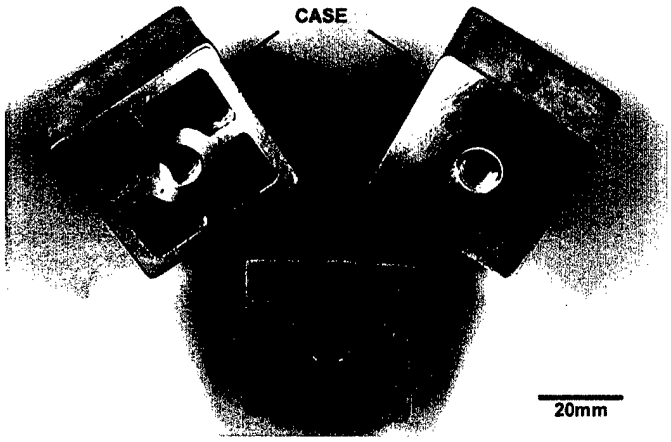

Figure 1. Photograph of machined BLR case and flange.

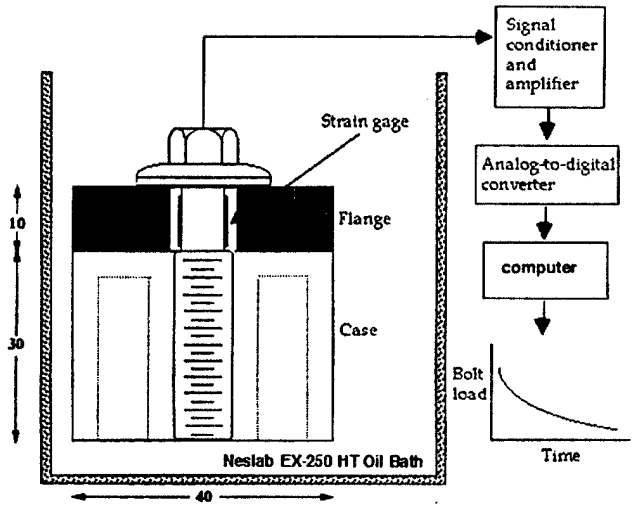

Figure 2. Schematic of the BLR test and data recording assembly; not to scale (dimensions are in mm).

and continuously acquired using the Measurements Group System 2000 analog-to-digital converter. Duplicate tests show repeatable results to within 3%. Slight differences in preload level, torque rate/method, and individual specimen properties (final machined state) are presumed to cause the modest variation that was observed.

AZ91D and AM50 specimens were also tested in this same manner but with the addition of up to three flat aluminum washers added to the assembly just beneath the bolt head. Aluminum washers had dimensions of approximately 10.6mm ID, 30.3mm OD, and 2.1mm thick. A single 1010 steel washer, of approximately the same dimensions (to within ±0.2mm) was placed under the bolt head in separate BLR tests.

Porosity levels of MEZ were evaluated using a precision Archimedes density method. Porosity levels of 2.8 and

Table 1. Chemical composition of HPDC Magnesium alloys MEZ, AE42, and AZ91D

Alloys	Composition (wt%)									
	Al	Zn	Mn	Si	Fe	Cu	Ni	RE total	Sn	Mg
MEZ	-	0.33	0.26	-	0.01	0.003	<0.001	1.92	-	Bal.
AE42	3.7	0.005	0.21	-	<0.005	0.003	0.005	2.69	-	Bal.
AZ91D	8.9	0.72	0.21	0.01	<0.005	0.004	<0.005	-	-	Bal.

* Rare earth (RE) consists of approximately 53%Ce, 25%La, 17%Nd, and 5%Pr.

3% for the BLR case and flange were measured. Microstructure was investigated using scanning electron microscopy (SEM) after etching in an ethylene glycol solution, transmission electron microscopy (TEM) after jet-polishing in a perchloric acid solution and ion-milling, and electron microprobe analysis (EMPA) after final polishing. Chemical composition of selected areas in the microstructure was analyzed by energy-dispersive spectrometry (EDS) and wavelength-dispersive spectrometry (WDS). Melting temperatures were investigated using differential scanning calorimetry (DSC). Duplicate tensile tests, carried out by Westmoreland Mechanical Testing and Research Inc., were performed at ambient and elevated temperatures on machined specimens of MEZ. Yield strength was determined by the 0.2% offset method. Strain rate was 0.005 mm/mm/min until yield and 0.05 mm/mm/min until failure according to ASTM E8-99 and E21-92.

RESULTS AND DISCUSSION

BOLT-LOAD RETENTION (BLR) BEHAVIOR - The decrease in bolt load of the torqued BLR assembly for MEZ is shown in Figure 3a. Here the instantaneous bolt load is normalized by the applied preload and plotted as a function of time at the indicated temperature. As shown in Figure 3b, MEZ demonstrates bolt-load retention behavior that is superior to other magnesium alloys tested in the same manner. It is notably better than AE42. For example, after an initial nominal preload of 28kN and exposure for 100h at 175°C, MEZ retained 78.5% of the initial load while AE42 retained only 55.5%.

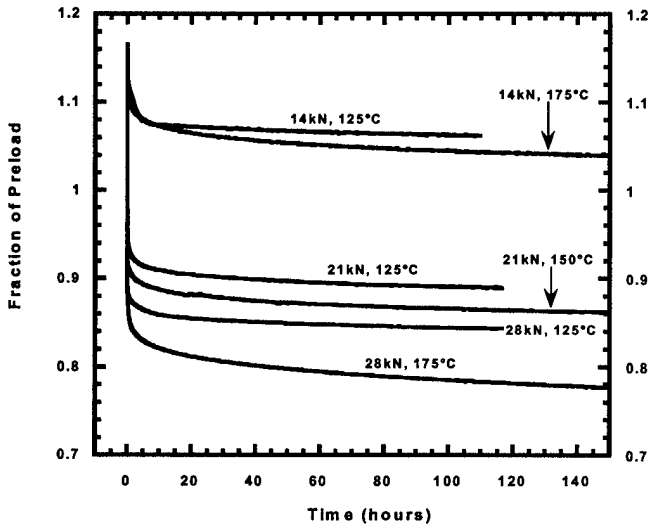

(a)

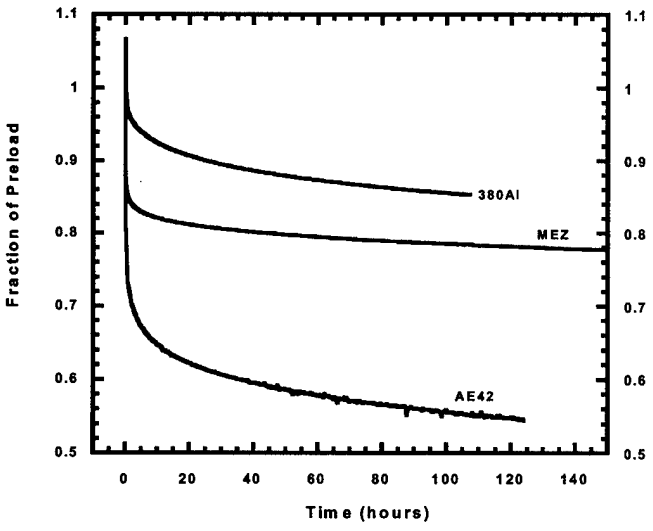

(b)

Figure 3. BLR curves of (a) MEZ at various temperatures and preloads and (b) MEZ, AE42, and 380Al BLR curves compared at 175°C, 28kN.

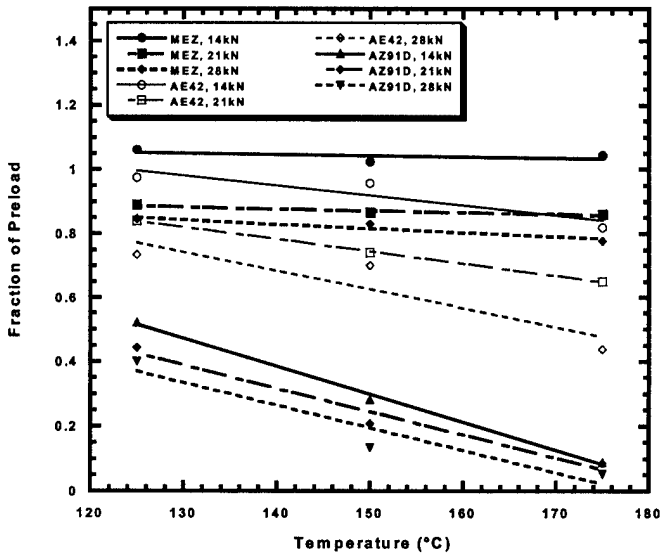

Figure 4. Comparison of BLR sensitivity to temperature (data represents retained load after 100 hours). AE42 and AZ91D data obtained from previous work [4].

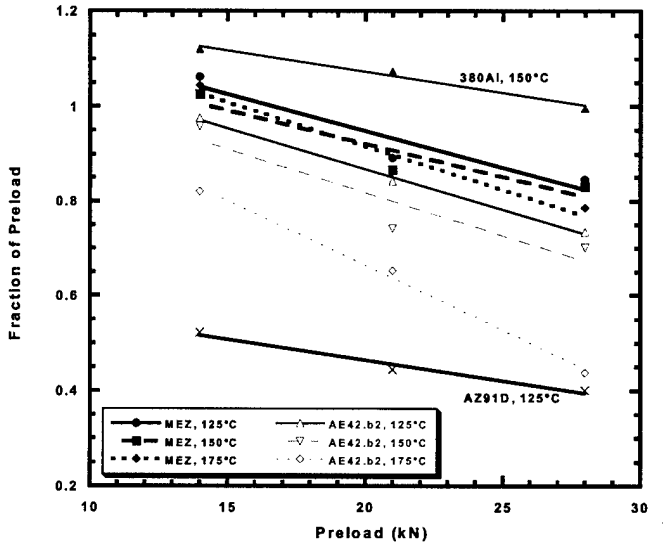

Figure 5. Comparison of BLR sensitivity to preload (data represents retained load after 100 hours). AE42 and AZ91D data obtained from previous work [4].

The dependence of BLR behavior on temperature and preload are shown for MEZ, AE42, and AZ91D in Figures 4 and 5. Unlike AZ91D and AE42, for MEZ there is little, if any, dependence of BLR on temperature for the preloads examined. As is observed for other alloys, the fraction of preload retained in MEZ decreases as the level of the preload increases, although its sensitivity to preload is not as great as for AE42, especially at 175°C.

The bolt-load retention behavior at very short exposure times is shown in Figure 6. Similar to AZ91D and AE42 [ref. 4,10], MEZ experiences an initial period of load increase caused by the thermal expansion mismatch between the magnesium case/flange and the steel bolt which is eventually countered by the onset of creep in the case/flange assembly. During this initial period, the steel bolt, having a lower thermal expansion coefficient, restricts the magnesium from expanding freely and imposes a greater compressive stress in the assembly. As expected, the initial load increase is greater at higher temperatures (greater thermal expansion effect) and lower preloads (lower stresses in the case/flange), with the preload level again showing a more pronounced effect than test temperature. At higher preloads, the initial loss of load is increased due to the higher compressive stresses in the assembly that result in an increase in creep deformation of the magnesium parts.

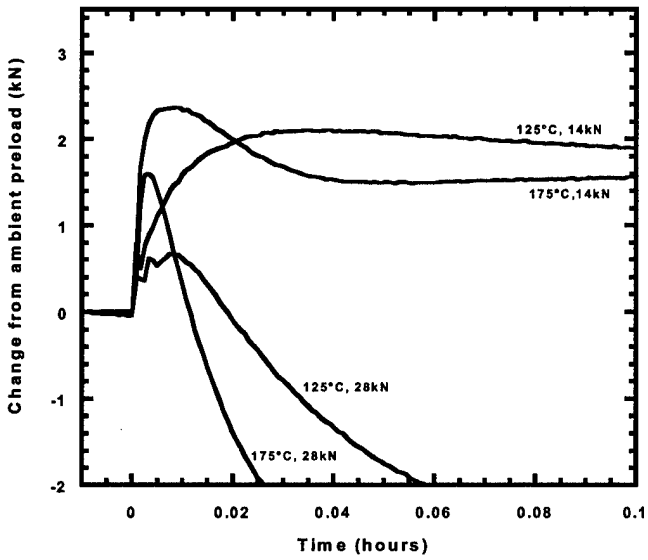

(a)

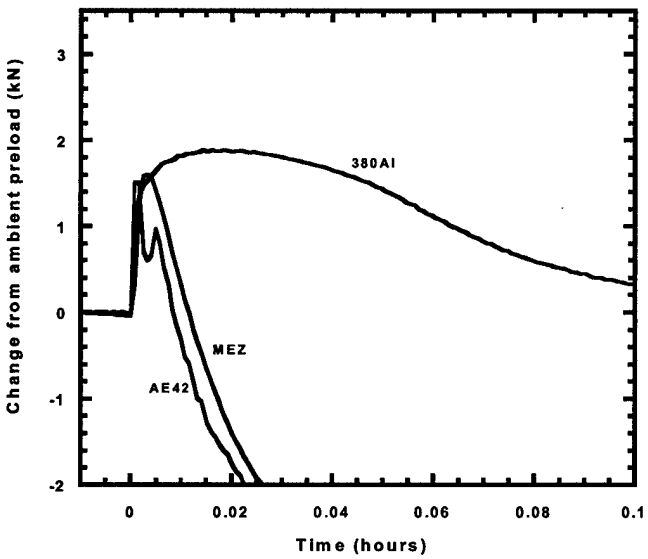

(b)

Figure 6. Initial transient response in bolt-load after submersion in oil bath (a) of MEZ at various temperatures and preload levels and (b) comparison of MEZ, AE42, and 380Al at 175°C, 28kN.

A bolt-load relaxation limit, F_r, above the lowest nominal preload of 14kN was displayed by MEZ at all temperatures and is extrapolated from the data presented in Figure 7. This value, representing the preload below which no stress relaxation occurs (bolt load drop of zero), is another representation of the superior creep resistance MEZ exhibits over other alloys. The initial thermal expansion of the alloy increases the bolt-load, as described earlier, and the alloy subsequently retains most of this load. MEZ exhibits this behavior even at 175°C, where its relaxation limit is 15.2kN in contrast to AE42 with F_r equal to 8.7kN.

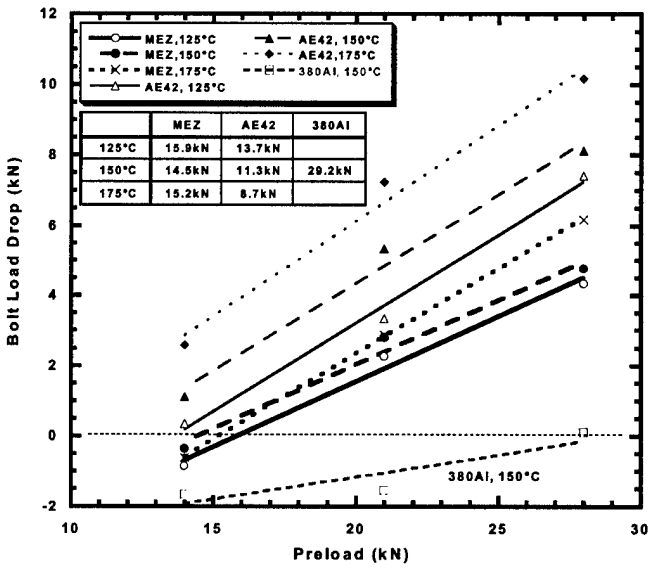

	MEZ	AE42	380Al
125°C	15.9kN	13.7kN	
150°C	14.5kN	11.3kN	29.2kN
175°C	15.2kN	8.7kN	

Figure 7. Drop from ambient preload after 100 hours at temperature as a function of ambient preload for MEZ, AE42, and 380Al. The bolt-load relaxation limit, F_r, which is extrapolated from this data, is included in the inserted table.

The relaxation limit, like the data shown in Figures 4 and 5, represents retained load after only 100 hours, but it is a good indicator of the behavior that a similar transmission case bolted-joint might display over its service life, and this is especially so for MEZ. Testing for over 200 hours at 175°C shows that the retained bolt-load was less than 2% lower (21.5kN) than at 100 hours (21.9kN). MEZ reaches a very shallow third stage stress relaxation period where further drop in bolt-load over time is minimal.

Similar to the BLR characteristics of other magnesium die casting alloys, MEZ displays an initial load increase followed by a considerable decrease in load (although this decrease is not as sharp as exhibited by other alloys), after which the load decreases at a fairly steady but gradual rate. This final, more gradual, state of load relaxation occurs when the stresses surrounding the bolt become less localized (in the upper end of the bolt) and more evenly distributed along the length of the threaded case. This has been analyzed by finite element modeling [16] and described in earlier reports on zinc and other magnesium castings [14,17]. Figure 8 shows the bolt-load MEZ retained after over 100 hours of exposure at different temperatures after a preload of 14, 21 and 28kN. A power law equation of the form $F(t)=ct^n$ can be used to describe the retained load in MEZ, with constants listed in Table 2. Except for the very early stage of the bolt-load test where there is a jump in the load as described in Figure 6, this power law depicts the BLR behavior of MEZ fairly well. For example, for 175°C and 28kN preload this equation would predict the retained load to be 21.6kN after 200h. The actual test resulted in a retained load of 21.5kN (< 0.5% error).

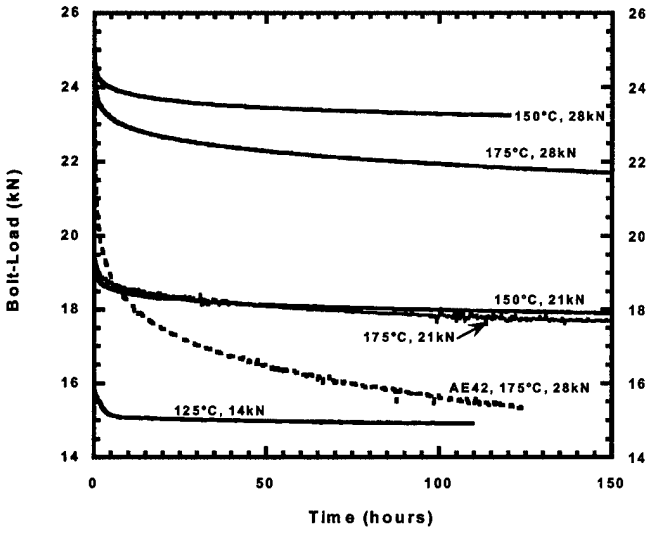

(a)

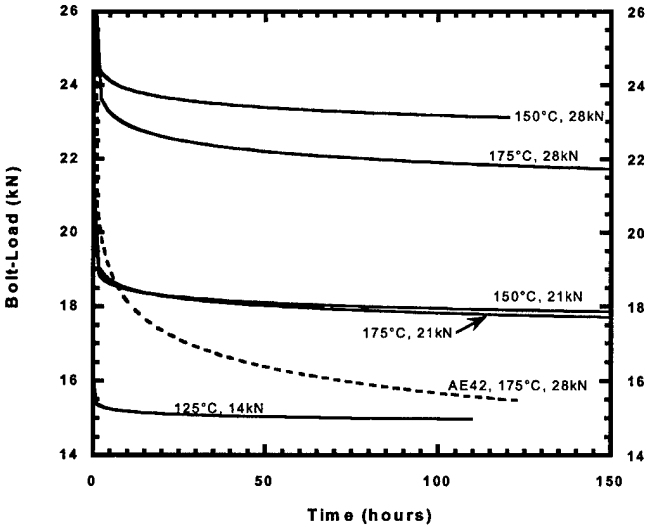

(b)

Figure 8. Retained bolt-load curves for MEZ at indicated preloads and temperatures (a) from experimental results and (b) described by the power law relationship, $F(t)=ct^n$. The AE42 BLR curve is added for comparison.

Table 2. Constants of the power law equation, $F(t)=ct^n$ for MEZ (AE42 data for 175°C, 28kN)

	125°C		150°C		175°C	
	c	n	c	n	c	n
14kN	15.39	-0.006	14.81	-0.004	15.45	-0.008
21kN	19.55	-0.013	18.98	-0.012	19.19	-0.016
28kN	24.89	-0.014	24.62	-0.013	23.98	-0.020
AE42					20.96	-0.063

TENSILE AND CREEP PROPERTIES – Results from duplicate tensile tests conducted on MEZ at RT, 125, 150, and 175°C are listed in Table 3 and compared to AE42 in Figure 9.

Figure 9 shows the variation of these properties with temperature compared to die cast AE42 tested previously in our laboratory. As shown, the yield and tensile strength for MEZ are lower than those measured for AE42 and decrease with increasing temperature. Elongation also increases with temperature to 150°C but decreases slightly at 175°C.

Table 3. Mechanical properties of die cast MEZ.

Temp. (°C)	YS (MPa)	UTS (MPa)	Elong. (%)
RT	97.6	134.8	2.9
125	83.6	115.9	6.8
150	78.0	110.0	7.5
175	73.5	99.7	5.0

Creep is known to occur at temperatures above approximately 0.4 of the absolute melting temperature of most metals. In alloys the melting range varies significantly depending on composition and the presence of higher melting phases. AZ91D, for example, begins to melt (solidus temperature, T_s) at approximately 475°C [18]. The onset of melting (T_s) for MEZ was determined to be 593°C by differential scanning calorimetry (DSC) This higher melting temperature is compared on an absolute basis with other alloys in Table 4, where it is evident that for the test temperatures of interest that MEZ is operating at a lower fraction of its absolute melting temperature.

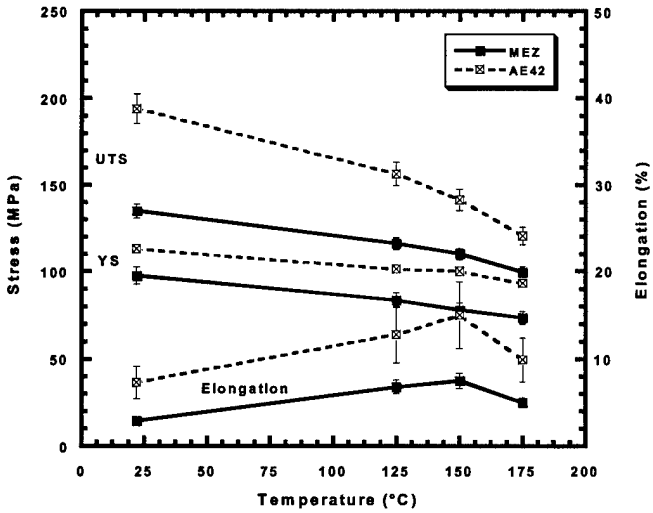

Figure 9. Mechanical properties of die cast MEZ and AE42 at various temperatures. (AE42-175°C data from previous work [11] obtained by crosshead displacement measurement)

Table 4. Homologous temperature values for die cast alloys. AE42, AZ91D, and 380Al data were obtained from previous work [18].

Test Temp. (°C)	MEZ T_s=593°C	AE42 T_s=613°C	AZ91D T_s=480°C	380Al T_s=540°C
125	0.46	0.45	0.53	0.49
150	0.49	0.48	0.56	0.52
175	0.52	0.51	0.59	0.55

MICROSTRUCTURE – With an absence of aluminum, MEZ lacks any Mg-Al or Al-RE phases. A Mg-RE phase exists and is partly responsible for the superior BLR behavior of the alloy. In a traditional sense, it can be expected that since grain boundary sliding commonly occurs during the creep of metals, a more coarsely grained microstructure is desired. However, with the introduction of stable precipitates along grain boundaries, grain boundary sliding at high temperatures can be impeded. WDS and EDS investigations using EMP and TEM, respectively, indicates that Mn is present within these grains of primary magnesium, and the rare earth elements and zinc are present along the grain and cell boundaries. A back-scattered SEM micrograph is shown in Figure 10, where the rare earth elements are shown in brighter contrast compared to the Mg matrix due to their higher atomic number.

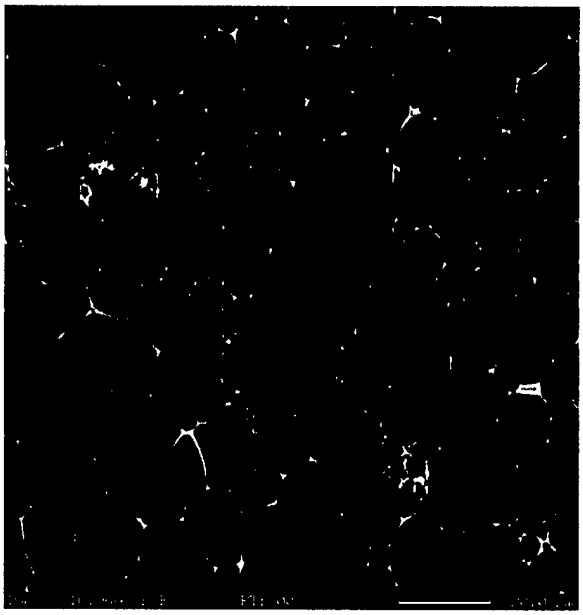

Figure 10. Electron microprobe back-scattered image of as-cast MEZ at 800x. The brighter grain boundary regions reflect the presence of the rare-earth elements in this phase.

The rare earth elements were introduced in this alloy as a mischmetal (MM) (with nominally 50% cerium and the remainder consisting of lanthanum, praseodymium, and neodymium) rather than separated rare earth metals since it is less costly but still effective as an alloying method [7, 8]. It is estimated that the presence of one or more stable Mg-RE phases along grain and cell boundaries in MEZ contributes greatly to its superior bolt-load retention behavior at elevated temperatures through intergranular and transgranular strengthening.

ROLE OF FASTENER GEOMETRY ON BLR – The geometry of the BLR test assembly was varied to determine the merits of an alternative means to an improved bolt-load assembly, through the addition of aluminum washers. Up to two aluminum washers were added to the BLR assembly of AZ91D and AM50, and 100-hour tests were conducted at different temperatures and preloads. These washers were placed under the M10 bolt head, in an effort to reduce the localized stress and, thus, reduce the creep occurring in the flange. Figures 11 and 12 offer a graphical representation of these results. As can be seen, the benefits of adding aluminum washers were normally very minimal, if not detrimental. At a low temperature (125°C) AZ91D showed a decrease in retained bolt-load with the addition of an aluminum washer and increased slightly with added washers, however the retained load was still below the retained load with no washer added. The expected variance is approximately 3% from test to test, so these differences are not considered significant. It is concluded that adding washers had no significant effect for these test conditions.

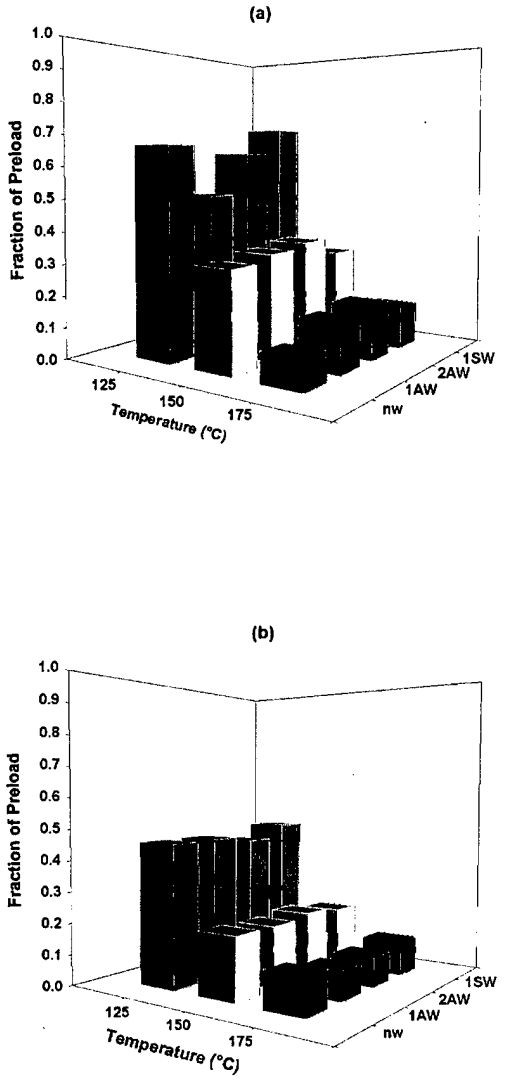

Figure 11. Bolt-load retention and the effect of adding washers to the BLR assembly of AZ91D at (a) 14kN and (b) 28kN. (nw = no washer, 1AW = 1 aluminum washer, 2AW = 2 aluminum washers, 1SW = 1 steel washer)

AM50 similarly displayed no significant improvement in retained bolt-load with the addition of aluminum washers. At a low preload (14kN) and temperature (125°C) adding aluminum washers increase the retained load only slightly. It is evident that at all other temperatures and preloads, the retained bolt-load is essentially unaffected by the addition of aluminum washers.

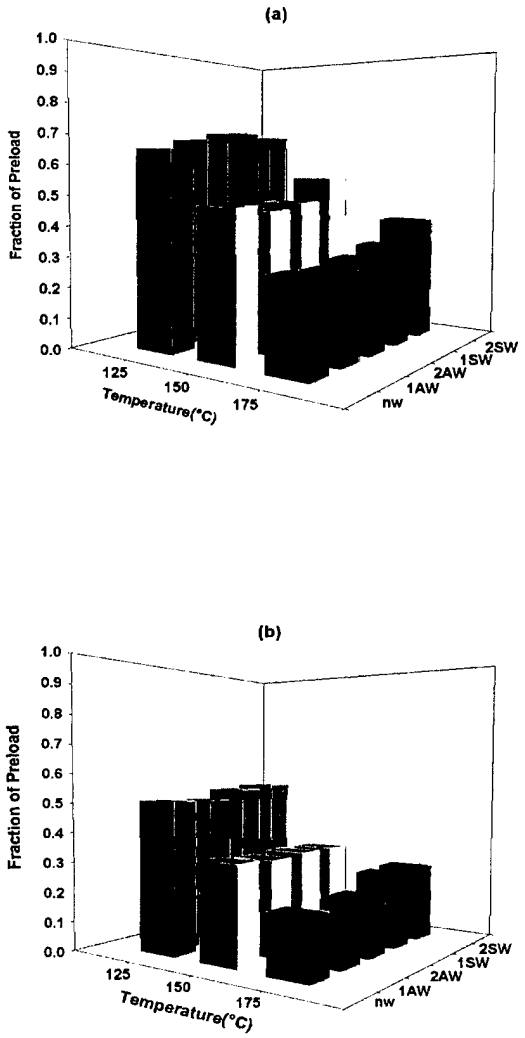

Figure 12. Bolt-load retention and the effect of adding washers to the BLR assembly of AM50 at (a) 14kN and (b) 28kN. (nw = no washer, 1AW = 1 aluminum washer, 2AW = 2 aluminum washers, 1SW = 1 steel washer, 2SW = 2 steel washers)

The aluminum washers may have crept slightly during the test, as washer deformation was visible after the tests, particularly at high preloads. With this deformation, the BLR assembly relaxes, as before. A single steel washer (up to two steel washers in the AM50 assembly) was added, separately, to the assembly to see if improved bolt-load retention prevailed. Deformation was not evident in the steel washers, however the BLR data obtained showed only a slight improvement by using a steel washer. These results did not appear to be statistically significant.

With the addition of washers, the effective length of bolt engagement decreases. This results in a greater induced load on the contact threads of the case, and thus increases the creep stresses. With the addition of every washer, approximately 1.5 contact threads were lost, and although the creep in the flange is further reduced as the stress on the flange face is more distributed, the loss of these threads works against the improvement of the stress-relaxation behavior. The amount of creep that occurs in the flange is not normally as significant as that which occurs in the case. Chen conducted studies on this with AZ91D and AE42 by separately replacing the magnesium flange or case with a stainless steel one. The relaxation limit for the stainless steel flange/magnesium case was normally lower than for the magnesium flange/stainless steel case, showing that, in most cases, more creep occurs in the threaded region of the case than at the flange/bolt-head interface [15]. Su, through the use of a finite element model, concluded that there is an uneven distribution of load at the early stages of the bolt-load retention test, with most of the stress initially localized in the upper threaded region [16]. However, this stress is more evenly distributed with time and the full thread contact area collectively contributes to opposing creep in that region [19].

Studies on the effect that increased bolt length has on the load-retention of zinc alloy pressure die castings were carried out by Murphy [17]. Results indicated that small increases in thread engagement length substantially improved the retained load. Through simulation, it was concluded that changing the contact area between the boss and the casting would have only a small effect on preload relaxation. Pettersen and Fairchild found substantial improvements in load retention by increasing the washer diameter and by increasing the thickness of the plate or the washer in the assembly [10]. However, they used a closed assembly, such that a nut was tightened at the end of the bolt. With increased thickness in the plate or washer, the effective bolt-length is increased, creating a combined effect that adds to the creep resistance of the clamping assembly. Such a closed assembly is not achievable in many drive train components, particularly in a typical automatic transmission case.

CONCLUSION

High pressure die cast MEZ displays far superior bolt-load retention behavior when compared to other magnesium alloys. The BLR characteristics of MEZ are nearly as good as those of 380Al even to temperatures as high as 175°C. The relatively high solidus temperature of MEZ and a stable microstructure containing higher melting rare earth phases contribute to its excellent creep resistance. Changes to the geometry of this particular bolt-load retention assembly by the use of washers did not improve the stress relaxation properties significantly as the thread engagement length of the case/flange and bolt was effectively decreased, resulting in greater creep in the BLR assembly. This last result indicates the importance of thread contact length for assemblies fabricated from magnesium alloys.

ACKNOWLEDGMENTS

I. Moreno thanks Carl Hendersen and Chris Palenik of the University of Michigan Electron Microscope Analysis Laboratory with help using the WDS and EDS on the EMP and TEM.

REFERENCES

1. J.F. King, "Development of Magnesium Diecasting Alloys". Paper presented at the Magnesium Alloys and their Applications conference, Wolfsburg, Germany. April 28-30, 1998, pp 37-47.
2. I. Nakatsugawa, S. Kamado, Y. Kojima, R. Ninomiya, and K. Kubota, "Corrosion of magnesium alloys containing rare earth elements." Corrosion Reviews, vol. 16, no. 1-2, 1998, pp 139-157.
3. J. Berkmortel, H. Hu, J.E. Kearns and J.E. Allison, "Die Castability Assessment of Magnesium Alloys for High Temperature Applications: Part 1 of 2", SAE Technical Paper 2000-01-1119, 2000.
4. K.Y. Sohn, J.A. Yurko, J.W. Jones, J.E. Kearns, and J.E. Allison, "Bolt-Load Retention Behavior of Die-Cast AZ91D and AE42 Magnesium", SAE Technical Paper 980090, 1998.
5. T.K. Aune and H. Westengen, "Property Update on Magnesium Die Casting Alloys", SAE Technical Paper 950424, 1995.
6. E.G. Sieracki, J.J. Velazquez, and K. Kabiri, "Compressive Stress Retention Characteristics of High Pressure Die Casting Magnesium Alloys", SAE Technical Paper 960421, 1996.
7. C.S. Roberts. Magnesium and Its Alloys. New York, John Wiley & Sons, Inc. 1960.
8. G.A. Mellor and R.W. Ridley, "Creep at 250°C and 300°C of Some Magnesium Alloys Containing Cerium", Journal of the Institute of Metals, vol. 81, 1952-53, pp 245-253.
9. P. Lyon, J.F. King, and K. Nuttall, "A New Magnesium HPDC Alloy for Elevated Temperature Use", Paper presented at the Proceedings of the 3rd International Magnesium Conference, Manchester, UK, April 1995, pp 99-108.
10. K. Pettersen and S. Fairchild, "Stress Relaxation in Bolted Joints of Die Cast Magnesium Components", SAE Technical Paper 970326, 1997.
11. K.Y. Sohn, J.W. Jones, and J.E. Allison, "Creep Mechanism in Die-cast Magnesium Alloys AZ91D and AE42", presentation made at the Automotive Alloys III, 1999 TMS Annual Meeting, San Diego, California, February 27-March 4, 1999.
12. J.H. Bickford. An Introduction to the Design and Behavior of Bolted Joints, 3rd Ed., New York, Marcel Dekker, Inc., 1995.
13. K.Y. Sohn, J.W. Jones, and J.E. Allison, "The Effect of Calcium on Creep and Bolt Load Retention Behavior of Die-Cast AM50 Alloy", Paper presented at the Magnesium Technology 2000, Nashville, Tn, March 12-16, 2000, pp 271-278.
14. K.Y. Sohn, J.W. Jones, J. Berkmortel, H. Hu, and J.E. Allison, "Creep and Bolt Load Retention Behavior of Die Cast Magnesium Alloys for High Temperature Applications: Part 2 of 2", SAE Technical Paper 2000-01-1120, 2000.
15. F.C. Chen, J.W. Jones, T.A. McGinn, J.E. Kearns, A.J. Nielson, and J.E. Allison, "Bolt-Load Retention and Creep of Die-Cast Magnesium Alloys", SAE Technical Paper 970325, 1997.
16. X. Su, K.Y. Sohn, D. Dewhirst, and J.E. Allison, "Finite Element Modeling of Bolt Load Retention of Die-Cast Magnesium", SAE Technical Paper 2000-01-1121, 2000.
17. S. Murphy and F.E. Goodwin, "Preload Relaxation of Steel Fasteners in Zinc Alloy Pressure Die Castings-Some Engineering Solutions", SAE Technical Paper 960763, 1996.
18. K.Y. Sohn, J.A. Yurko, F.C. Chen, J.W. Jones, and J.E. Allison, "Creep and Bolt-Load Retention Behavior of Die-Cast Magnesium Alloys", in Automotive Alloys II, San Antonio, Tx, TMS, February 16-19, 1998, pp 81-90.
19. X. Su, Personal communication.

Microstructural Characterization Of A Die Cast Magnesium-Rare Earth Alloy

I.P. Moreno[1], T.K. Nandy[1], J.W. Jones[1], J.E. Allison[2], and T.M. Pollock[1]
[1]University of Michigan, Materials Science and Engineering, Ann Arbor, MI 48109, USA
[2]Materials Science Department, Ford Motor Co., Dearborn, MI 48126, USA

Keywords: Magnesium; Die Casting; Scanning/transmission electron microscopy (STEM); Electron diffraction; Electron microprobe analysis

Abstract

Microstructural characterization of high-pressure die cast alloy MEZ (Mg-2.5RE-0.35Zn-0.3Mn) reveals equiaxed cells of α-Mg with a partially divorced interdendritic eutectic. Detailed diffraction studies coupled with WDS analysis shows the presence of a continuous $Mg_{12}RE$ intermetallic phase in the eutectic aggregate along with fine MgO particles.

Introduction

Low-cost high-temperature magnesium alloys have evoked a renewed interest in recent years because of their potential for automotive applications in the form of die cast components [1,2]. Microstructural stability and creep strength remain major challenges in the development of these alloys, and different alloying additions have been made to attain superior room and elevated temperature properties. Aluminum as an alloying addition has maintained considerable use [3] as it improves castability, by increasing fluidity and freezing range, and room temperature tensile properties, by solid solution strengthening and precipitation of a β intermetallic ($Mg_{17}Al_{12}$). However, at high temperatures the beneficial effects of Al appears to diminish because of microstructural instabilities that lead to either coarsening of the massive β intermetallic [4,5] or precipitation of discontinuous β from supersaturated Mg [6]. Addition of rare earth (RE) elements, resulting in the formation of a fine Al_4Re intermetallic as in AE42 (Mg-4Al-2RE), alleviates this problem to a large extent. However, the problem of instability may persist above 150°C, where decreased creep strength has been observed [7,8]. It has also been suggested that a decomposition of Al_4RE to Al_2RE and $Mg_{17}Al_{12}$ occurs at 175°C, resulting in the deterioration of creep properties [8]. Therefore, the presence of aluminum in Mg alloys may introduce instability problems and reduce creep resistance at elevated temperatures.

Recently, a new composition of magnesium-rare earth alloy (Mg-2.5RE-0.35Zn-0.3Mn), which does not contain Al [9], has been developed. The alloy, designated Elektron MEZ, exhibits superior high temperature creep and stress retention behavior compared to that of the benchmark alloy AE42 [9,10]. Although reasons for such improvement are still being investigated, the stability of grain boundary phases may be partly responsible for this effect.

Recent work by Bettles and coworkers [11] has concentrated on the interdendritic phase in the sand cast version of this alloy that they have determined to be $Mg_{12}(La_{0.43}Ce_{0.57})$. A detailed microstructural study in the die casting condition, which may be expected to be different considering the higher solidification rates, has not yet been reported. As most of the applications of magnesium alloys in automotive applications employ die-casting, an understanding of the microstructure in die cast alloys is important. The present research characterizes the microstructure of Elektron MEZ in high-pressure die cast condition. The study forms a part of a larger program designed to evaluate the high temperature mechanical behavior of the MEZ alloy where the stability of microstructure becomes a vital issue [7].

Experimental

MEZ was melted at 700°C under an SF_6 cover gas and pressure die cast in a 450 ton B&T cold chamber machine with the die temperature maintained at 177-232°C. Gate velocity was approximately 30m/s for each of the four die cavities. The alloy was analyzed for chemical composition using ICP atomic emission spectroscopy and the results are shown in Table 1.

TABLE 1
Chemical composition (wt.%) of HPDC MEZ

RE total**	Zn	Mn	Fe	Cu	Ni	Mg
1.92	0.33	0.26	0.01	0.003	Traces	Bal.

** Rare earth (RE) consists of about 53%Ce, 25%La, 17%Nd, and 5%Pr

As cast specimens were polished with 1-μm diamond suspension and etched with ethylene glycol. Back-scattered electron (BSE) images of the polished specimens were obtained using a Phillips XL30 FEG SEM. The chemical compositions of the phases were determined with a Cameca CAMEBAX electron microprobe analyzer. Thin foils for transmission electron microscopy were prepared using a Fishione twin jet polisher in a perchloric acid-methanol solution at –30°C. Subsequently, low angle ion milling was employed to remove the surface oxide layer introduced during jet polishing. A Philips scanning transmission electron microscope (CM-12) was used for examination of microstructure. Selected area electron diffraction (SAED) patterns from different zone axes were recorded and the online software Electron Microscopy Image Simulation (EMS) was used for the simulation of the diffraction patterns.

Results

The as cast microstructure of MEZ is represented in Figure 1 where an equiaxed granular structure is generally observed. Occasionally, cells with a higher aspect ratio and fully developed dendrites are also observed. However, the microstructure is mostly uniform with the predominance of equiaxed regions. Mn is present in solid solution while traces of Zn and RE elements were registered during EMPA/WDS. A continuous phase can be clearly seen at the cell boundaries in the BSE image in Figure 1b, where the brighter contrast is reflective of the presence of heavier rare earth elements. EDAX analysis also shows enrichment of rare earth elements in these areas, although the regions are too fine to accurately determine chemical composition. However, recent work on sand cast MEZ [11], where the microstructure is considerably coarser, indicates that the grain boundary phase is $Mg_{12}Ce$ with some substitution of other rare earth elements for Ce. Anticipating the same phase in the die cast alloy, a sample was exposed for 24 hours at 589°C taking care that the eutectic temperature was not exceeded (reported as 592°C for the $Mg \rightarrow \alpha Mg + Mg_{12}Ce$ transformation [12]). As expected, coalescence of

the grain boundary phase occurs with particles 10-20μm in diameter, allowing accurate compositional analysis by EMP/WDS. The composition determined is shown in Table 2, along with that of the matrix. The composition of the second phase is close to that reported by Bettles *et al.* on sand cast MEZ [11].

TABLE 2
Chemical composition (at.%) analysis by electron microprobe analysis

	Mn	Zn	Ce	La	Nd	Pr	Mg
Matrix	0.117	0.033	0.007	-	0.003	-	99.84
2nd phase	0.073	1.187	3.400	3.913	-	0.003	91.37

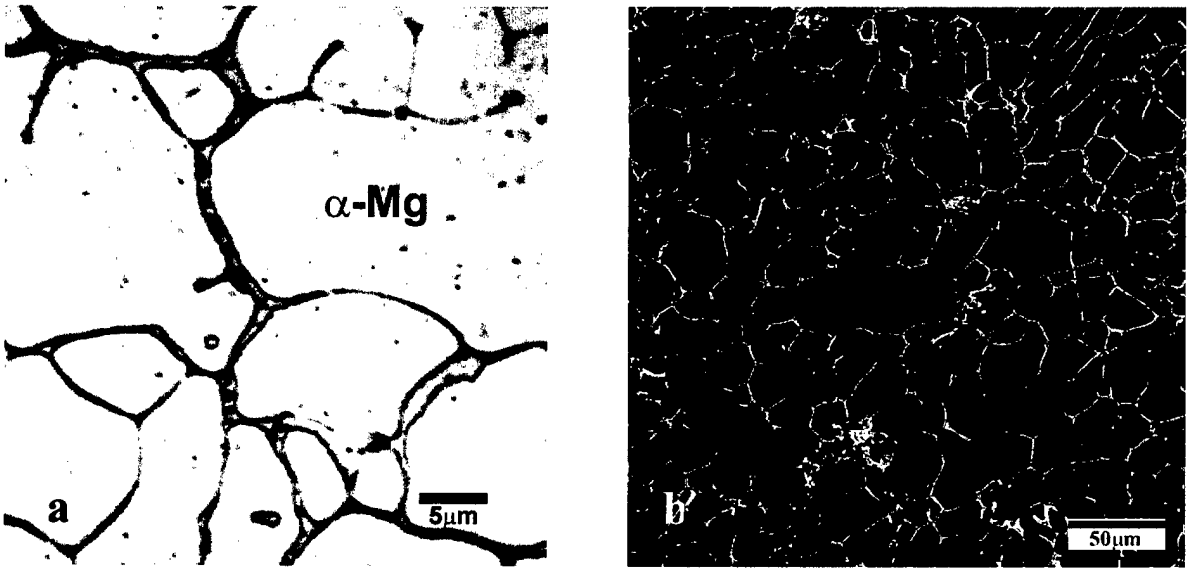

Figure 1. (a) Optical and (b) BSE micrographs of as-cast MEZ describing the different microstructural features in the die cast condition

A transmission electron micrograph of the as cast alloy is shown in Figure 2a. The grain interior is single-phase α-Mg with no observed precipitation of second phases. The grain boundary region is a single phase with occasional embedded dark particles that do not change contrast while tilting. A diffraction pattern corresponding to the grain boundary phase is shown in Figure 2b. The pattern can be indexed to the [101] zone axis of the $Mg_{12}Ce$ intermetallic with a tetragonal crystal structure and space group of I4/mmm. Several diffraction patterns have been recorded in different orientations and consistently indexed to $Mg_{12}Ce$, just as reported for sand cast MEZ [11]. The intermetallic shows sub-boundaries in different locations and is heavily faulted, as shown in Figure 3a. The corresponding [131] zone axis diffraction pattern (Figure 3b) shows streaked diffraction spots that likely result from these faults. The calculated lattice parameters of the intermetallic phase are a=1.016nm and c= 0.588nm. TEM/EDAX was attempted for compositional analysis of the fine particles (100nm diameter) embedded in the grain boundary, but accurate results could not be obtained because of the interference of the surrounding Mg-RE intermetallic. Diffraction patterns recorded from the small dark particles (Figure 4) show ring patterns, indicating a nanocrystalline phase, that have been indexed to MgO. The volume fraction of the oxide particles varies form region to region. A companion work [7] describing the high temperature creep behavior of HPDC MEZ shows that the

microstructure remains stable after 350 hours of steady-state creep at either 60 or 80MPa at 175 or 150°C, respectively.

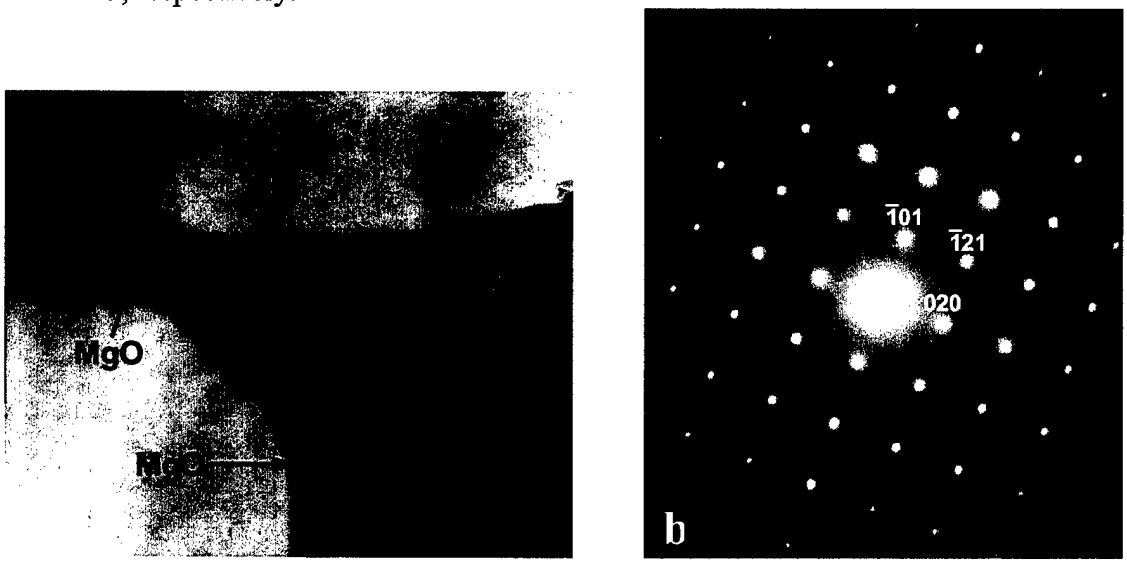

Figure 2. (a) TEM micrograph of the grain boundary phase in as-cast MEZ and (b) grain boundary phase SAED pattern - [101] zone axis.

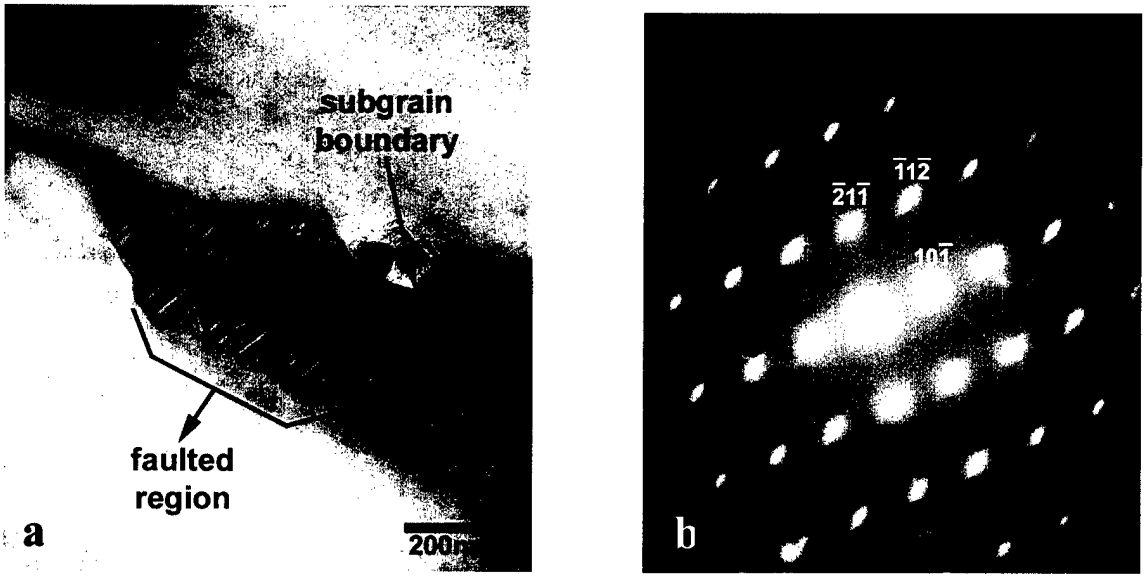

Figure 3. (a) TEM micrograph of faulting and sub-boundaries in the grain boundary phase and (b) corresponding SAED pattern showing streaking – [131] zone axis.

Discussion

Since the binary phase diagrams of Mg with Ce, La, Pr and Nd (the rare earth elements) are similar in the Mg rich end, the Mg-Ce equilibrium diagram (Figure 5) can be examined for understanding the solidification behavior of these alloys. The vertical line in the phase diagram shows the approximate composition of this alloy. Normally during equilibrium solidification, as the alloy cools and approaches the liquidus, primary dendrites of α-Mg solidify first and subsequent secondary and ternary branches develop. However, owing to the large cooling rates

and turbulent nature of solidification during die-casting, well-defined dendrites were not observed.

The eutectic structure, developed during the final stages of solidification, appears divorced, just as found in other Mg-Al [13] and Mg-Al-Zn alloys [14]. The divorced structures observed in these alloys have been attributed to the large undercooling of liquid below the eutectic temperature that results in a shift of the liquid composition away from the coupled zone for eutectic growth. A tendency for transition from a lamellar to a divorced eutectic morphology increases with decreasing Al and an increasing cooling rate. Since the present study employs high-pressure die-casting, the appearance of a divorced eutectic structure is, therefore, not surprising. The presence of fine MgO particles may be attributed to precipitation of Mg during eutectic solidification and subsequent oxidation during jet polishing. Thus, while the microstructure appears completely divorced at low magnification, high magnification TEM shows regions of a two-phase aggregate indicating a partially divorced eutectic structure, although the fraction of α–Mg and, therefore, MgO is very small. Thus, the solidification behavior of MEZ is similar to those observed in other Mg-Al hypoeutectic alloys. Table 3 compares microstructures of some commonly used die cast Mg alloys.

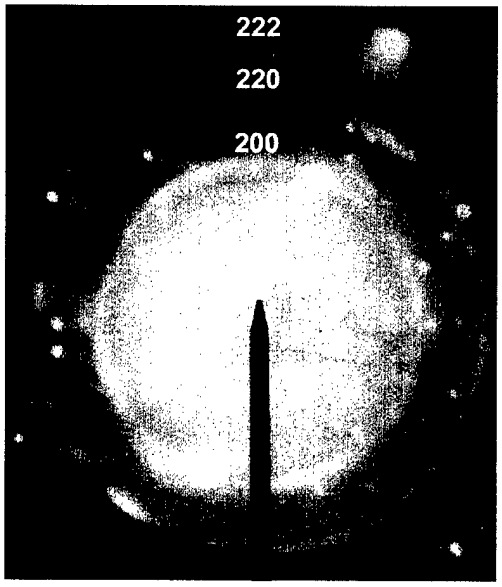

Figure 4. SAED pattern of fine particles in the grain boundary phase.

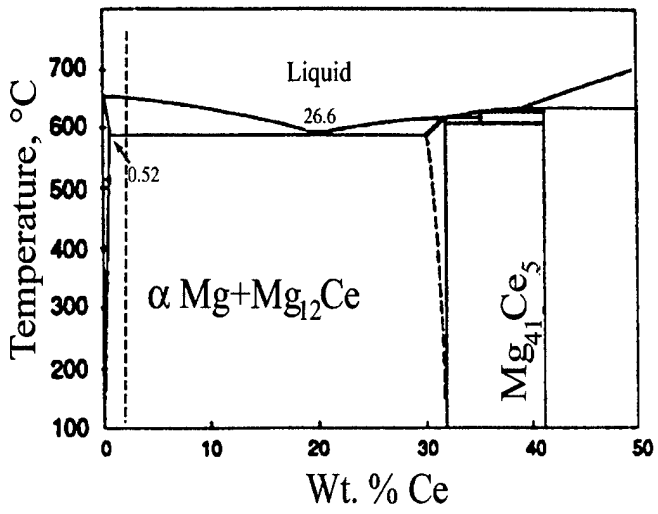

Figure 5. Binary Mg-Ce phase diagram [12] with approximate alloy composition shown by the dashed vertical line.

TABLE 3
Microstructure of die cast magnesium alloys.

Alloy (nominal wt%)	Phases present	Microstructure	Ref.
AZ91D (Mg-9Al-1Zn-0.2Mn)	αMg+β $Mg_{17}Al_{12}$	α dendrites + divorced eutectic (α/β)	14
AS21 (Mg-2Al-1Si-0.02Zn-0.2Mn)	αMg+β $Mg_{17}Al_{12}$ + Mg_2Si	α dendrites + divorced eutectic (α/β) +Chinese script Mg_2Si	14
AE42 (Mg-4Al-2RE-0.05Zn-0.1Mn)	αMg+Al_4RE	α dendrites + lamellar eutectic (α/AL_4RE)	3
MEZ (Mg-2.5RE-0.3Zn-0.35Mn)	αMg+$Mg_{12}RE$	α dendrites + partially divorced eutectic (α/$Mg_{12}RE$)	Present study

Conclusions

1. The microstructure of high-pressure die cast Mg-rare earth alloy MEZ consists of primary equiaxed α–Mg cells (occasionally developed dendrites) with a partially divorced eutectic aggregate at the cell boundaries.
2. A continuous $Mg_{12}RE$ intermetallic constitutes the eutectic regions with small amounts of MgO originating from the precipitation of Mg during eutectic solidification.
3. The presence of the predominant cellular structure and divorced eutectic can be attributed to the large undercooling and turbulent nature of solidification during die-casting.
4. The solidification sequence in MEZ is similar to that observed in other hypoeutectic magnesium alloys containing Al and can be explained using a typical Mg-Ce binary phase diagram.

Acknowledgements

The authors are grateful to Dr. Carl Henderson of the University of Michigan Electron Microscope Analysis Laboratory (EMAL) for his help in EMPA. Also the financial support provided by Ford Motor Company is gratefully acknowledged.

References

1. J. F. King, Magnesium Alloys and their Applications, Eds. K.U. Kainer, Wiley- VCH, New York, p. 15 (2000)
2. P. Humble, Materials Science Forum, 21, 45 (1997).
3. D. J. Sakkinen, SAE Paper 940779 (1994).
4. G. Raynor, The Physical Metallurgy of Magnesium Alloys and its Alloys, Pergamon Press, New York (1959).
5. Y. Guangyin, S. Yangsha, and D. Wenjiang, Scripta Mat., 43, 1009 (2000).
6. M.S. Dargusch, G.L. Dunlop and K. Petterson, Magnesium Alloys and Their Applications, Eds. B.L. Mordike and K.U. Kainer, Werkstoff-Informationsgesellschaft, Frankfurt, Germany, p. 277 (1998).
7. I.P. Moreno, J.W. Jones, and J.E. Allison, research not yet published (2001).
8. B. R. Powell, V. Rezhets, M. P. Balogh and R. A. Waldo, Magnesium Technology 2001, Ed. J. Hryn, The Minerals, Metals and Materials Society, p. 175 (2001).
9. P. Lyon, J. F. King and K. Nuttall, Proc. of the 3rd International Magnesium Conf., 99 (1996).
10. I.P. Moreno, K.Y. Sohn, J.W. Jones, and J.E. Allison, SAE Paper 2001-01-0425 (2001).
11. C.J. Bettles, C.J. Rossouw and K. Venkatesan, Magnesium Alloys and their Applications, Eds. K.U. Kainer, Wiley- VCH, New York, p. 131 (2000).
12. "Alloy Phase Diagrams", ASM Handbook Vol.3, ASM International, Materials Park, OH, 1992.
13. M.D. Nave, A. K. Dahle and D. H. StJohn, Magnesium Technology 2000, Eds. H.I. Kaplan, J. Hryn and B. Clow, The Minerals, Metals and Materials Society, p. 233 (2000).
14. M.D. Nave, A. K. Dahle and D. H. StJohn, Magnesium Technology 2000, Eds. H.I. Kaplan, J. Hryn and B. Clow, The Minerals, Metals and Materials Society, p. 243 (2000).

Creep Behavior of a Die Cast Magnesium-Rare Earth Alloy

I.P. MORENO, J.W. JONES, and J.E. ALLISON

The tensile and compressive creep behavior of experimental HPDC alloy, MEZ, shows significant improvement over benchmark alloy AE42 and other magnesium alloys under development for high temperature automotive applications. Improved high temperature creep resistance is attributed to a stable, continuous $Mg_{12}RE$ intermetallic phase much different in morphology than the intergranular phase found in AE42 and other Mg-Al alloys. The role of microstructure on the short and long term mechanical response is heavily influenced by the presence of aluminum in Mg alloys, and the superior creep performance of this alloy is largely attributed to its absence. Tensile and compressive creep behavior is uniform and correlates with the bolt-load retention behavior of this alloy. Thermal and mechanical properties are related to the different stages of creep in MEZ.

I. INTRODUCTION

The trend toward magnesium as a material choice in automobiles has been gradual, increasing from 3lbs to about 8lbs over the past decade for a typical vehicle, compared to almost 250lbs of aluminum per vehicle in 2000[1]. Mg provides potential for significant weight savings as experienced in the aerospace industry, but a greater barrier exists in the automotive industry where affordable alloys are restricted to low temperature applications. In recent years, there has grown a renewed interest in exploring the high temperature creep behavior of commercial alloys

and the development of new Mg alloys. What progress has shown is that perhaps "more" is not necessarily "better." This paper will describe the superior performance of one such alloy.

Most magnesium alloys used in die casting are based on a Mg-Al system because aluminum increases strength, improves castability and surface finish, and is relatively cheap. It has high maximum solubility in Mg at the eutectic temperature (~12wt%), but additions are limited to about 9wt% to avoid brittleness. AZ91D (Mg-9wt%Al-1wt%Zn), has remarkable mechanical properties and has been the workhorse of Mg die cast alloys[2,3,4]. In these Mg-Al alloys, a hard eutectic β-$Mg_{17}Al_{12}$ phase forms that improves tensile strength with increased volume fraction, although at the cost of ductility. For applications requiring increased ductility and impact resistance, Mg alloys AM60 and AM50, with substantially lower levels of Al, are employed. This β phase also improves corrosion resistance by covering and protecting grain boundary regions typically susceptible to chemical attack[4]. AZ91D and AM50/60 are known to creep above 100°C[5], and this has been correlated with their poor compressive stress retention at elevated temperatures[6,7]. Although experiencing lower transient creep[7,8], AZ91D displays substantially greater long-term creep deformation than for other Mg-Al alloys with lower levels of Al, and the trend is similar among other AM and AZ alloys[9]. This behavior has been attributed to the microstructural development in these Al-containing alloys.

The development of the β-$Mg_{17}Al_{12}$ phase in Mg-Al alloys has been reported to reduce creep resistance although its role is still under debate. Some support that the β phase coarsens and softens during high temperature creep, resulting in extensive grain boundary sliding[4,10,11,12,13] while others describe β as maintaining its room temperature hardness up to 275°C and improving

creep resistance[2,14,15]. For the latter, the loss in creep resistance is conversely attributed to the discontinuous precipitation of β-$Mg_{17}Al_{12}$ in areas of highly supersaturated α-Mg near grain boundaries, where the increased presence of lamellae provides more surfaces on which sliding can occur[2,9], and the migration of a high angle grain boundary ahead of a growing precipitate colony aids grain boundary sliding[16]. The continuous transgranular precipitation that develops and coarsens is not an effective barrier to dislocations slipping on the basal plan since its morphology consists of small cross section thin plates parallel to the basal plane[2,9]. Homogenization heat treatments can help reduce the segregation experienced during die casting, however porosities inherent to high-pressure die cast (HPDC) alloys are known to result in excessive surface blistering when heat treated. Therefore, attempts have been made to introduce alloying elements that could essentially capture excess aluminum through the formation of desired compounds.

When die cast, the addition of small amounts of silicon to Mg alloys has the effect of producing a fine dispersion of Mg_2Si along grain boundaries, enhancing creep resistance by reducing grain boundary sliding[17,18]. AS41 (4wt%Al-1wt%Si) was developed in the late 1960s with a slightly improved creep resistance over AZ91D, and AS21 (2wt%Al-1wt%Si) was later developed with improved creep resistance over AS41 although with poor castability because of the decrease in Al[18,19]. Sakkinen attributed the marginal creep resistance of the AS alloys to the softening of the massive $Mg_{17}Al_{12}$ compound at elevated temperatures which negates the benefits of Mg_2Si[18].

The benefits of alloying Mg with rare-earth (RE) elements were discovered as early as the 1930s and subsequent research has stressed that a less costly alloying method of adding a mixture of rare earth elements (approximately 50wt%Ce and the remainder La, Nd, and Pr) is equally effective in resisting creep and has been used extensively[3,20,21,22]. Excess Mg_9Ce, likely referring to the more recently identified $Mg_{12}Ce$ intermetallic, appeared in semiglobular form at grain boundaries, blocking grain boundary sliding and migration instrumental in the creep of high purity Mg[21]. This would require other higher energy processes to provide the intergranular adjustment during high temperature creep, such as non-basal slip, to which tertiary creep in these alloys was attributed. RE elements also reduce the corrosion rate of Mg alloys[23] and increase the fluidity during casting of Mg-Al alloys by reducing the freezing range[24]. The addition of small amounts of Mn to RE-containing alloys improves corrosion resistance, strengthens the cast material, increases the solubility of Ce that allows for greater precipitation, and restricts the growth of the Mg_9Ce particles during precipitation[2,10,18,25]. This precipitation is continuous, unlike the large volume of the discontinuous β-$Mg_{17}Al_{12}$ precipitate that develops during the creep of Mg-Al alloys. Concern for maintaining strength and castability resulted in a Mg-Al-RE alloy that gave potential for high temperature automotive applications.

AE42 (4wt%Al-2wt%RE) came to be the automotive industry's benchmark alloy suggested to be viable for use in powertrain components, especially transmissions operating below 150°C[26]. The formation of $Al_{11}RE_3$ (or Al_4RE) at grain boundaries where RE represents Ce or other rare earth element substitutions as has been determined by others[18,27,28], provides improved creep resistance over the AZ, AM, and AS alloys[27]; higher levels of aluminum (~9wt%) resulted in the formation of the mass Mg-Al eutectic phase found in AZ91. AE42's superior stress retention

and creep properties over AZ91D were demonstrated by several[6,7,29,30] although marginal performance was demonstrated above 150°C. The decrease in creep strength from Mg-RE alloys is partly attributed to the more favored formation of Al-RE compounds. Also, there still exist areas of Al-rich Mg(SS) near the grain boundaries where as much as 6-7wt%Al concentrations are found[27]. It is this segregation that may lead to the subsequent undesired precipitation of $Mg_{17}Al_{12}$. It has also been reported that Al_4RE becomes unstable at temperatures above 150°C and decomposes into Al_2RE and $Mg_{17}Al_{12}$, both of which are detrimental to creep resistance[31]. As for other RE-containing alloys, there is an increased cost associated with AE42, although it has been determined that the operating costs for casting and trimming AE42 would be similar to that of AZ91D if manufactured in comparable volumes[32]. Small strontium additions improves the creep resistance of AE42 as there is a virtual elimination of supersaturated α-Mg through the formation of Al-Sr grain boundary phases[2,33], but the high cost of Sr may unacceptable for automotive applications. Many over the last several years have pioneered the development and investigation of alternative Mg alloys to AE42.

The addition of small amounts of low-cost calcium (<1wt%) to die-cast AM50 greatly improves high temperature properties as has been demonstrated in creep and bolt-load retention testing[34,35] and has been attributed to the formation of high melting Al_2Ca at the grain boundaries restraining grain coarsening and boundary sliding[36]. However, castability problems limit the level of Ca to below 0.3wt%, resulting in inferior performance to AE42[32]. In other developments, the presence of 8%Zn has overcome the degraded castability problems associated with increased Ca, and improved creep resistance has been attained[37]. However, with these

very high levels of zinc added to moderate levels of Al a considerably higher density results, sacrificing one of magnesium's major advantages.

More recently, GM has reported excellent creep performance, although stress levels are unknown, from high Ca-containing Mg-Al (plus <0.3wt% Sr and/or Si) alloys in the absence of Zn[38], where a hexagonal, thermally stable intergranular $(Mg,Al)_2Ca$ phase presumably restricts grain boundary sliding during creep[39]. Mg_2Si particles or Sr may also contribute to creep resistance. Although high in Ca and absent of Zn, two traits known to be highly detrimental to the castability of Mg alloys, these alloys have been reported as having excellent castability for small parts, based on the absence of surface cracking[40]. Related work on thixomolded Mg-Al-high Ca alloys determined the eutectic compound was not Al_2Ca but more likely Mg_2Ca and $Mg_{17}Al_{12}$ (or possibly a ternary Mg-Al-Ca compound)[41]. It is apparent that further investigation and high temperature/stress stability demonstrations are needed in these alloys.

Other alloy developments have included the addition of 2.6wt% rare earth metals to a Mg-5.3wt%Al-2wt%Ca-0.17wt%Mn alloy (ACM552) that has been incorporated into Honda's 80mpg hybrid cars[42]. Al-Ce phases are reported to provide creep strengthening by inhibiting grain boundary sliding, although Al-Ca and Mg-Ca compounds were said to be present as well. Additions of small amounts of high-cost Sb has also improved tensile yield strength and creep rupture life of permanent mold cast AZ91 by refining the β-$Mg_{17}Al_{12}$ phase and grain size, while hindering the mobility of dislocations by slow diffusing Mg_3Sb_2 precipitates straddling grain boundaries and penetrating some grains[13].

It is apparent that the presence of aluminum in Mg alloys, although beneficial to strength and castability, is detrimental to high temperature creep performance. Alloying techniques have fallen short or need further demonstration in suppressing the shortcomings of Mg-Al alloys while maintaining good castability. In 1996, Magnesium Elektron (Manchester, UK) developed a new alloy, designated Elektron MEZ, and reported creep properties superior and yield strength and corrosion resistance similar to AE42 up to 177°C[43]. This new alloy contains no aluminum but castability was demonstrated in a range of components including a filter housing, gearbox, and oil pan. As reported in the past[21,22,44,45,46], alloys based on the Mg-Zn-rare earth light alloy system have exhibited good creep resistance at elevated temperatures (even at 200°C). The addition of zinc, as described earlier, improves the fluidity and castability as well as provides effective solid solution and precipitation hardening to low Al-containing alloys[2]. Recent studies on the bolt-load retention (BLR) behavior of HPDC MEZ demonstrated superior performance to other magnesium alloys tested (notably AE42 and AM50+ 0.88wt%Ca), nearly as good as 380Al at 175°C under high stress[47]. Similar results on the superior bolt-load retention properties over AZ91D has been reported on sand-cast MEZ[48]. The purpose of this paper is to report the creep properties of HPDC MEZ and investigate the microstructural features that may provide insight to the superior high temperature/high stress creep properties of this die cast alloy.

II. EXPERIMENTAL

MEZ, with a nominal composition of Mg-2.5%RE-0.35%Zn-0.3%Mn, was pressure die cast in a 450-ton B&T cold chamber machine at Mag-tec Casting Corporation (Jackson, MI). Using a four-cavity die, each set of test specimens used in creep and bolt-load retention (BLR) testing

were produced. Melt and die temperatures were 700-710°C and 177-232°C, respectively, with sulfur hexafluouride (SF_6) used as a cover gas. Gate velocity was 28.3 m/s for the creep specimens. The actual composition of as-cast MEZ, obtained by inductively coupled plasma (ICP) atomic emission spectroscopy and mass spectrometer on a fatigue specimen is given in Table I along with the compositions of materials from other studies[29,49]. Here, RE represents the total wt% of rare-earth elements Ce, La, Nd, and Pr.

Microstructure was investigated using optical and scanning electron microscopy (SEM) and electron microprobe analysis (EMPA) after 1-micron diamond suspension final polishing where etching in an ethylene glycol solution was used for when needed. Transmission electron microscopy (TEM) was used after jet polishing in a perchloric acid solution and subsequent ion milling at a 5-7° incident angle to remove an oxidation layer formed during polishing. Grain size was determined using the line intercept method as well as through image analysis. Volume fraction of second phase was estimated through image analysis. Chemical composition and phase identification was conducted using energy-dispersive spectrometry (EDS), wavelength-dispersive spectrometry (WDS), and electron diffraction as described in other published work[50]. Thermal exposure was conducted at 590°C/24hrs, naturally cooled, encapsulated in vacuum under an argon atmosphere to avoid heavy oxidation. Porosity levels of MEZ were evaluated using a precision Archimedes density method and selective region porosity volume fraction was estimated through image analysis. Melting temperatures were investigated using differential scanning calorimetry (DSC) where the solidus temperature was taken as the first increase in heat flow with increasing temperature. DSC testing was conducted in a Perkin-Elmer DSC-7 where

either alumina or carbon fiber pans were used, yielding matching results in each case. Nitrogen was used as a cover gas during each test.

Cylindrical subsize tensile bars were used in creep testing, in accordance with ASTM B577. Threaded grips and fillet sections were machined from the cast bars to accommodate the test frames. Approximately 0.5 mm of the die cast skin was removed from the gage section to eliminate its influence on mechanical properties as was done to the machined BLR specimens to simulate the final machined state of a typical automatic transmission housing. Final dimensions were approximately a 5.72 mm diameter and 31.75 mm gage length, as determined through the use of a shadowgraph in accordance with ASTM E139. Compressive creep specimens were cut from the gage section of the creep bars and machined to a final length of 17.15 mm giving a length to diameter ratio of 3 to 1.

Duplicate tensile tests, carried out by Westmoreland Mechanical Testing and Research Inc., were performed at ambient and elevated temperatures on machined specimens of MEZ. Yield strength was determined by the 0.2% offset method. Strain rate was $0.083ks^{-1}$ until yield and $0.83ks^{-1}$ until failure according to ASTM E8-99 and E21-92. Creep testing was performed on constant load creep frames with fixed lever arms, and strain was measured with two LVDTs coupled with a digital data-acquisition system, giving a strain resolution of about $1.5x10^{-5}$. Samples were stabilized at temperature (±1°C) for several hours before testing at constant temperatures ranging from 125 to 175°C for tensile creep tests and at 150°C for compressive creep tests. Initial applied stresses ranged from 50-100MPa in tension and up to 150MPa in compression. To ensure steady-state creep had been reached, tests ran for up to 1000 hours; steady-state creep

rates were determined using a 15-point linear regression sliding function to provide a strain-rate versus time curve, as shown in Figure 1, and observing the minimum creep rate in this curve. The practice of determining the steady-state creep rate through linear regression of the appropriate linear region in the strain versus time curve gave adequate approximation to the minimum creep rate, also shown in Figure 1, and this method was used when analyzing creep data with very low creep rates. These two methods have shown to differ insignificantly, roughly 5-10% in previous work[51].

III. RESULTS

A. *As-Cast Microstructure*

The general microstructure of as-cast MEZ can be seen in Figure 2a, where an equiaxed granular structure of α-Mg is found along both the transverse and longitudinal sections of the specimen gage. Occasionally, patches of cells with a higher aspect ratio are apparent in various regions, as shown in Figure 2(*b*), and rarely more fully developed dendrites are found, as shown in 4(*c*). During die casting, dendrites may not always develop fully because of the very high solidification rates. The magnesium dendrites (or cells) found in die castings typically display multiple orientations resulting from the turbulent nature of solidification during die casting[52]. The cell boundary, then, is considered equivalent to a grain boundary although its influence on mechanical behavior may be different. The average interdendritic spacing of MEZ was 10.4μm ± 0.8μm. The α-Mg contains manganese in solid solution (0.26wt%), and traces of Ce and Zn (<0.1wt%) are present as well. No apparent precipitation within the primary α-Mg matrix was observed.

A relatively continuous second phase, determined as $Mg_{12}RE$ and described in other work[50] fills the interdendritic region. This multi-faulted phase, shown in Figure 3, has different features that are accented in (*a*) optical, (*b*) secondary scanning electron, and (*c*) transmission electron microscopy images. Occupying a volume fraction of roughly 16%, this interdendritic phase contains the majority of the rare earth elements present in MEZ and is represented by the spectrum in Figure 4(*a*) and can be compared to the primary α-Mg matrix phase spectrum in 4(*b*). This phase coalesced substantially, as shown in Figure 5, after thermal exposure at 590°C for one day but retained its composition and crystal structure. This second phase remained stable during creep testing at all temperatures and stresses, as its continuous nature is shown relatively unchanged in Figures 6 and 7.

As will be described in the next section on thermal analysis, it is expected that there exists a Mg-$Mg_{12}Ce$ type eutectic and would be the first to melt upon heating. A partially divorced eutectic is apparent in this alloy as the continuous $Mg_{12}RE$ phase maps out the grain boundaries. As can be seen in Figures 3a and 3c, a dispersion of very fine particles appears along the grain boundaries and they were determined to be MgO during TEM investigation. It is not certain whether these MgO particles formed during casting or during sample preparation. It is likely that the $Mg_{12}RE$ phase, saturated in Mg upon solidification, precipitated Mg particulates upon further cooling. The dark disc-shaped particles in the interdendritic region in Figure 3a may be the precipitated Mg, giving a partially divorced eutectic phase and forming oxides during jet polishing.

A representation of the casting defects present in MEZ is shown in Figure 8. An average porosity level of 2.7% was calculated for the creep specimens through density measurements, however much of these defects existed in the grip sections of the test bars. As shown in Figure 8b, a presence of intergranular cracking or hot tearing was found in this cast alloy ranging in size from only a few microns to one millimeter. The average volume fraction of porosity in the gage section of the test bars was approximately 0.5%.

B. *Relative Operating Temperature*

The solidus temperature for MEZ was determined to be 593°C by DSC, as shown in Figure 9. This temperature and corresponding homologous temperatures, T/T_s, are compared to other alloys in Table II. It is evident that, for the test temperatures of interest, MEZ is operating at a relatively low fraction of its absolute melting temperature. AE42 operates at a slightly lower homologous temperature because of its slightly higher T_s, although it has been reported elsewhere[4,18] that AE42 has a much lower solidus temperature than that determined in this effort. Under equilibrium conditions, a Mg-Ce binary alloy would undergo a eutectic reaction at 592±2°C yielding a Mg-$Mg_{12}Ce$ eutectic phase, thus it is expected that the first phase to melt is the divorced Mg-$Mg_{12}RE$ eutectic present in this alloy.

C. *Mechanical Properties*

Yield strength, tensile strength, and ductility for MEZ as a function of temperature are shown in Table III. The strength is significantly low when compared to published properties of many Mg-Al alloys[12,18]. The room temperature ductility, measured as the percent elongation upon failure, is comparable to that of AZ91D and ACM522. Figure 10 compares these properties to those of

AE42, where it is seen that both alloys experience a decrease in strength with temperature, while ductility increases with temperature to 150°C and slightly decreases at 175°C. Yield and tensile strength of MEZ is substantially lower than that of AE42 and other Mg-Al alloys at all temperatures and will help explain the difference in the initial behavior this alloy displayed when compared to AE42 during creep testing.

C. *Creep Behavior*

1. *General trends - tensile creep*

The tensile creep behavior of MEZ is shown in Figure 11. An initial elastic/plastic deformation and primary creep region was observed that is more pronounced at higher initial stresses and temperatures. A clear transition to secondary creep is observed, particularly at stresses below 80MPa. This differs from that found in Mg alloys with low creep resistance such as AZ91D, AM50, and AM50 with low calcium additions (<0.6wt%) as described in previous work[36]. It is apparent from these creep curves that even well above the reported yield strength at temperature, little strain is experienced after the instantaneous and primary creep strain. For example, at 150°C at an initial applied stress of 90MPa (more than 10MPa above the reported YS), after an initial strain of 1.6% and 0.96% subsequent primary creep strain only a 0.07% increase in strain occurred after over 400 hours of steady-state creep. At 175°C, stage III or tertiary creep is reached much earlier when the initial stress is near or exceeds the yield strength (<15 hours at 90MPa). When the creep behavior is compared to that of AE42 as is shown in Figure 12, it is clear that these two alloys present similar creep response at a low temperature and stress (ie. 125°C at 60MPa), shown as coincident curves in Figure 12. However, at higher temperatures and stresses, the creep response is very different. The initial instantaneous strain observed upon

Figure 15 shows the influence of temperature on $\dot{\varepsilon}_{min}$ at a constant stress. A clear transition in the minimum creep rate response to temperatures is observed above 150°C. The activation energy for creep (Figure 15) for low temperatures (<150°C) is quite low, suggesting that the mechanism for creep is not thermally dependent in this temperature range for MEZ. Above 150°C, the apparent activation energy increases substantially ranging from 112 to 321 kJ/mol, depending on the initial applied stress. This behavior is similar to that observed for AE42[49]. The activation energy of AE42 also displayed a dependence on temperature and a clear transition was reported at 150°C above 70MPa. In this higher temperature region, the activation energy was reported as 301 and 411 kJ/mol at 80 and 90MPa, respectively.

3. *Compressive creep behavior*

The general compressive creep behavior was characterized and is compared to that of samples tested in tension in Figure 16. The creep response is very similar in both testing directions in that an instantaneous elastic/plastic deformation is followed by a short primary creep period that transitions to stage II creep. Only for tests of very high initial stresses (>90 MPa) did the tension and compression creep behavior differ. This is to be anticipated since tensile failure modes are not present in compression. Compressive creep tests on MEZ were conducted at stresses up to 150MPa, a stress equivalent to that experienced during typical bolt-load retention tests[53]. Stage III (tertiary) creep was not observed for any compressive stress condition for the time periods tested.

The very low strains observed during compression creep are attributed to the low creep rates experienced during secondary creep. The stress exponent under compression creep was calculated to be 4.6 over the entire stress range. Compared to tensile creep behavior in Figure 17, there is no apparent transition creep response as compressive stress increases. Figure 18 shows the differences in compressive creep behavior comparing MEZ and AE42. The minimum creep rate of MEZ is as much as two orders of magnitude lower than AE42 at 120MPa. AE42 displays a great increase in stress dependence above 80MPa where the reported stress exponent rises from 1.3 to 13. It is clear that MEZ has a superior creep resistance at very high stresses, which is also reflected in its superior bolt-load retention properties reported elsewhere[47]. The overall compressive creep behavior is described and compared in Figure 19. The creep behavior is very similar between these two alloys at low stresses. Similar to loading in tension, there is a greater initial elastic/plastic deformation in MEZ, after which the creep strain is almost identical. However, at very high stresses MEZ transitions to a much lower minimum (steady-state) creep very quickly. AE42, on the other hand, experiences greater creep strains over longer creep times and, thus, displays inferior creep resistance for extended high temperature applications.

IV. DISCUSSION

A. Summary of key results

The solidus temperature of MEZ is comparatively high, reducing the relative operating temperature it experiences during creep testing when compared to alloys showing poor creep resistance, such as AZ91D. This is important in reducing the mobility of dislocations, as a higher melting point alloy will better resist dislocation climb mechanisms. However, yield and

tensile strength, as well as the instantaneous and primary creep response, of MEZ is shoddy when compared to other commercial Mg alloys. The long-term creep behavior, similar to its stress retention behavior, particularly at higher temperatures and stresses, is superior to AE42 and other recently developed Mg alloys with viability for high temperature automotive structural applications. It is of interest to the alloy developer, therefore, to understand the typical modes of creep deformation in Mg and the altering of these caused by microstructural variations resulting in improved creep behavior.

B. Creep of magnesium and the influence of microstructure

Roberts[54] described the plastic creep strain in fine-grained Mg by the summation of two components: transient creep, associated with transgranular deformation, and steady-state creep, associated with grain boundary deformation. At elevated temperatures grain boundary deformation plays a greater role in the creep process, particularly during steady state creep[10]. The applied stress was critical by causing the alternation of grain boundary sliding or shearing and the subsequent migration of them for granular adjustment as the localized strain energy increased. Quantity of grain boundary area is, then, important in the creep of magnesium. A discontinous type of precipitation, favorable in Mg-Al alloys, increases this area three-fold[55]. It is critical, therefore, to establish a favorable microstructure in Mg that remains stable at elevated temperature and stress. Whether a grain boundary phase such as $Mg_{17}Al_{12}$ softens or decreases its effect in resisting creep at elevated temperatures and/or a discontinuous precipitation in Al-saturated α-Mg during elevated creep contributes to increased grain boundary sliding, it is apparent that the long term creep resistance of Mg depends on a stable, preferably continuous, grain boundary phase that inhibits plastic deformation.

C. Role of aluminum on microstructural development and short and long term mechanical response in magnesium

The interdendritic phases of MEZ and AE42 have very different morphologies. The interdendritic phase in MEZ (see Figure 3), unique to other non-Al containing Mg-Ce, Mg-RE, and Mg-RE-Zn alloys[20,22,55,56,57,58], consists of a continuous interdendritic phase. In contrast, a discontinuous interdendritic phase (Al_4RE or $Al_{11}RE_3$) in die cast AE42 is embedded in a continuous α-Mg matrix highly saturated in Al in this region. This phase is often referred to as a lamellar eutectic, but its morphology is quite different. The degeneration of a typical lamellar eutectic is common under rapid solidification where the formation of the eutectic is secondary (ie. primary α-Mg solidification followed by the secondary solidification of a small amount of remaining liquid)[59]. This is typical of a divorced eutectic that results in the formation of intermetallics with various shapes around the primary α-Mg solid solution phase. An example is shown in Figures 20 and 21, where the Al_4RE strengthening phase in AE42 is discontinuous while the α-Mg phase is continuous throughout the microstructure.

There is a general trend showing greater strength and lower initial creep strain in magnesium alloys with increased levels of aluminum. The short term strength of Mg-Al alloys has been attributed to the high solubility of aluminum[19] in magnesium which provides substantial solid solution strengthening. In the same respect, Al solute atoms can segregate to dislocations and inhibit their motion, thereby reducing creep strain. AE42 and MEZ display quite different ambient and elevated tensile properties, as described earlier. At all temperatures, both the yield strength and ultimate tensile strength were greater in AE42. The instantaneous plastic

deformation and subsequent transient creep is greater in MEZ when compared to AE42 as well, which correlates with the observed differences in yield strength. This is similar to the behavior seen in Mg-Al alloys with a lower content of aluminum than that of AZ91D. AZ91D generally shows greater strength over other alloys such as AS41, AS21, and AE42[18,60,61] and also shows a smaller instantaneous deformation and transient creep than these other alloys[8,62]. During the solidification of AE42, of the initial ~4wt% of aluminum approximately 3wt% is left in solution assuming that all the rare earth elements bind to aluminum, forming AL_4RE ($Al_{11}RE_3$)[27]. Much of this remaining aluminum has been noted to segregate towards the grain boundaries where concentrations of up to 6-7wt% are found. This aluminum remaining in solution explains the higher yield and tensile strength in AE42, but it may also partially explain why its creep resistance deteriorates at higher temperatures.

It has been found in this effort and in others[31,40,47], that the long-term creep resistance of AE42 is deficient at temperatures above 150°C. The solubility of Al in Mg decreases from about 10wt% at the eutectic temperature to 2-3wt% at 200°C[27], so these areas of segregated Al in die cast AE42 may be expected to precipitate (perhaps in the form of the β-$Mg_{17}Al_{12}$ compound if there are no more rare earth elements available) when exposed to elevated temperatures (ie. above 150°C). A dramatic decomposition of the lamellar Mg-Al_4RE eutectic to one dominated by a particulate Al_2RE phase and traces of lamellar Al_4RE and $Mg_{17}Al_{12}$ precipitates at 175°C was reported by Powell[31] but has not been confirmed in this work As described earlier, the presence of a discontinuous phase provides more surfaces for which sliding may take place and this may lead to a decrease in creep resistance at elevated temperatures. MEZ has a continuous interdendritic strengthening intermetallic phase, as described earlier, that would be expected to

inhibit grain coarsening and grain boundary sliding and pose an obstacle for the migration of dislocations generated during creep. This intermetallic phase, being of an $Mg_{12}RE$-type, is present in high volume fraction even with a very low overall level of rare earth elements since there is a much greater ratio of Mg atoms per atom of rare earth elements (12:1).

D. Stability of microstructure

The stability of microstructure during high temperature creep is an important part of an alloy's ability to resist deformation. As mentioned, although the $Mg_{17}Al_{12}$ β-phase in AZ91 contributes to its room temperature strength and low temperature creep resistance by providing an obstacle to dislocation motion, this phase is reported to soften or decompose when the material is heated up to high service temperatures[4,52]. For the test conditions used, the microstructure of MEZ appeared to remain stable. There is no evident change in morphology or volume fraction of the intergranular phase described earlier. The as-cast and crept microstructures of MEZ are both shown in Figures 6 and 7. Figure 6(*b*) shows the microstructure of MEZ after being crept at 175°C with an initial stress of 60MPa; the micrograph was captured after approximately 350 hours of steady-state creep. Figure 7(*b*) captures the apparently unaffected interdendritic phase after roughly 350 hours of steady-state creep at 150°C with an initial stress of 80MPa.

When investigating the stability of microstructure in AE42, a more noticeable change in morphology of the grain boundary phase occurs at higher stresses and creep temperatures. In related work, the eutectic phase in AE42 changes morphology at higher stresses (85MPa) at 150°C, as shown in Figure 20(*b*) and compared to the as-cast state in 20(*a*), due to the diffusion of the narrow eutectic cell boundary, resulting in higher creep strains[52]. Shown in Figure 21(*b*),

the intergranular eutectic phase after thermal exposure at 175°C with an initial tensile stress of 70MPa appears coarser than in the as-cast state shown in Figure 21(*a*), although more modest than the thermally driven transformation given by Powell[31] and described earlier. In that study, the nature of the creep test conducted was not reported; the observed transformation is expected also to be stress dependent. Roberts reported that with an increase in stress, an increase in the volume fraction of the discontinuous precipitation during creep of Mg-Al alloys is observed, and similar acceleration of this precipitation as a result of plastic deformation have been reported previously[55]. Furthermore, it has been demonstrated[9,27] that Al_4RE does not coarsen nor change morphology after creep periods of up to 100 hours at 250°C-50MPa. Thus, it is expected that observed changes in AE42's morphology and subsequent decrease in creep resistance be attributed to not only the elevated temperature environment but also the applied stress.

E. Stress/temperature dependence of the minimum creep rate and creep mechanisms in Mg

The period of minimum or steady state creep rate during dislocation creep processes describes the balance between dislocation pile up and entanglement and the recovery and further motion of those dislocations that is experienced during tertiary creep. It is apparent in MEZ that $\dot{\varepsilon}_{min}$ increases substantially above 150°C, which would indicate that creep recovery mechanisms are heightened in this higher temperature range. The stress dependence of steady-state creep, yielding a stress exponent in the range of 5.6-7.2 at lower tensile stresses, falls close to that found for highly creep-resistant Mg alloy QE22 (n=7)[63] where the rate-controlling mechanism was dislocation glide. Creep mechanisms based on dislocation motions on basal and non-basal planes have been reported for AZ91D at higher stresses where stress exponents of 5.4 to 6.9 were reported for 180 and 150°C respectively[39]. Vagarali and Langdon[64] reported that at higher

stress levels where the stress exponent is close to ~6.0, there is evidence of non-basal slip. It is possible, therefore, that for this stress region (<90MPa from 125-150°C, <70MPa at 175°C) MEZ experiences dislocation glide in the basal plane as well as dislocation cross-slip from basal to prismatic planes. In early studies, dislocation motion on the basal plane of Mg has been reported for low temperatures ($<0.6T_m$) while non-basal cross slip has been observed at higher temperatures and low stress[10,65,66], however non-basal slip has been suggested in Mg-Ce alloys at lower temperature where the blocking of grain boundary sliding and migration is prevented by the Mg-Ce grain boundary precipitate, necessitating higher energy processes to provide the intergranular adjustment[21]. Shown in Figure 22 are dislocations that appear to be on the basal plane near the grain boundary in MEZ after roughly 350 hours of steady-state creep at 150°C with an initial stress of 80MPa. As observed in other regions of its microstructure, there are no apparent dislocation subgrain networks as would be expected where a dislocation climb process was the rate controlling mechanism during steady-state creep. Further analysis is needed to confirm these initial findings.

No clear explanation has been proposed for the very high activation energies measured in this study, although they have been reported for other Mg-RE alloys[67,68]. In Mg-RE alloys investigated by Henning[69], a proposed mechanism including extensive non-basal slip (ie. a cross from basal to prismatic planes), with an activation energy of 250kJ/mol, could account for the higher values obtained. Although grain boundary sliding may be inhibited by the continuous $Mg_{12}RE$ phase, it cannot be concluded that grain boundary sliding would not at least partially account for creep deformation. It can be expected that different mechanisms are contributing to the creep process and the resultant activation energy is additive. At high stresses and

temperatures, the growth of existing cracks and the behavior of casting defects may influence creep rates and calculated stress exponents and activation energies. Further TEM dislocation analysis on as-cast and crept MEZ is needed for a matured understanding of the dominant deformation mechanisms and rate controlling processes prevailing during creep.

V. CONCLUSIONS

The mechanical and creep testing of HPDC MEZ under the conditions described, the limited microstructural analysis performed, and the review of some literature of various Mg-alloys lead to the following conclusions:

1. The superior short-term response of AE42 and other high Al-containing Mg alloys both in tensile and creep testing is attributed to the presence of aluminum, which has high solubility in Mg and provides substantial solid solution strengthening.
2. The long-term creep behavior of MEZ is superior to AE42 and other Mg-Al alloys at elevated temperatures and stresses. This is attributed to the lower steady-state creep rates observed.
3. MEZ's creep resistance displays a low sensitivity to temperature, particularly below 150°C.
4. A continuous interdendritic intermetallic phase, similar to $Mg_{12}Ce$, provides creep strengthening and remains stable at elevated temperatures, more so than the eutectic phase found in Al-containing Mg alloys.

5. The discontinuous nature of the Al_4RE (or $Al_{11}RE_3$) intermetallic embedded in a continuous matrix of α-Mg significantly enriched in solute aluminum accounts, in part, for the inferior creep resistance of AE42 at elevated temperatures and stresses.
6. Magnesium alloys in which aluminum is absent show promise in improving the high temperature creep performance of HPDC components while maintaining acceptable castability.

ACKNOWLEDGMENTS

The University of Michigan acknowledges the financial support of this research by Ford Motor Company.

REFERENCES

1. K. Buchholz: *Automotive Engineering International*, 2000, pp 44-45.
2. M.S. Dargusch: *PhD Thesis, The University of Queensland*, 1998.
3. C.S. Roberts: *Magnesium and its Alloys*, John Wiley & Sons, Inc., New York, 1960
4. A. Luo and M. Pekguleryuz: *Materials Science*, 1994, vol. 29, pp. 5259-5271.
5. C. Suman: *SAE paper 910416*, 1991.
6. F.C. Chen, J.W. Jones, T.A. McGinn, J.E. Kearns, A.J. Nielsen, and J.E. Allison: *SAE paper* 970323, 1997.
7. K.Y. Sohn, J.A. Yurko, F.C. Chen, J.W. Jones, and J.E. Allison: *Automotive Alloys II*, 1998, pp. 81-90.

8. P. Zhang, R. Agamennone, W. Blum, B. Grossman, and H. Haldenwanger: *Magnesium Alloys and their Applications*, 2000, pp. 716-721.

9. P. Humble: *Materials Forum*, 1997, vol. 21, pp. 45-56.

10. G. Raynor: *The Physical Metallurgy of Magnesium and its Alloys*, Pergamon Press, New York, 1959.

11. J. Waltrip: *Proc. 47th Annual World of Magnesium Conf.*, 1990, pp. 124-129.

12. T. Aune and H. Westengen: *SAE paper 950424*, 1995.

13. Y. Guangyin, S. Yangshan, and D. Wenjiang: *Scripta Materialia*, 2000, vol. 43, pp. 1009-1013.

14. M. Fukuchi and K. Watanabe: *Journal of Japan Inst. Of Metals*, 1975, vol. 39, p. 493.

15. W. Sequeira, M. Murray, and G. Dunlop: *Proc. 3rd Int. Magnesium Conf.*, 1997, p. 63.

16. M.S. Dargusch, G.L. Dunlop, and K. Pettersen, *Magnesium Alloys and their Applications*, 1998, pp. 277-282.

17. J. Hillis and S. Shook: *SAE Paper 890205*, 1989.

18. D.J. Sakkinen: *SAE Paper 940779*, 1994.

19. W.E. Mercer II: *SAE Paper 900788*, 1990.

20. T.E. Leontis: *Journal of Metals*, 1949, vol. 1, pp. 968-983.

21. C.S. Roberts: *Journal of Metals*, 1954, vol. 6, pp. 634-640.

22. G.A. Mellor, *Journal of the Institute of Metals*, 1952-53, vol. 81, pp. 245-253.

23. I. Nakatsugawa, S. Kamado, Y. Kojima, R. Ninomiya, and K. Kubota: *Corrosion Reviews*, 1998, vol. 16, pp. 139-157.

24. Y. Lu, Q. Wang, X. Zeng, W. Ding, C. Zhai, and Y Zhu: *Materials Science and Engineering*, 2000, A278, pp. 66-76.

25. O. Holta, M. Vedem, and D. Albright: *Trans. NADCA 18th Int. Die Casting Congress and Exposition*, 1995.

26. A. Luo: *Magnesium Technology*, 2000, pp. 89-97.

27. G. Pettersen, H. Westengen, R. Hoier, and O. Lohne: *Materials Science and Engineering*, 1996, A207, pp. 115-120.

28. L.Y.Wei, G.L. Dunlop, and H. Westengen: *Materials Science and Technology*, 1996, vol. 12, pp. 741-750.

29. K.Y. Sohn, J.A. Yurko, J.W. Jones, J.E. Kearns, and J.E. Allison: *SAE Paper 980090*, 1998.

30. K. Pettersen and S. Fairchild: *SAE paper 970326*, 1997.

31. B. Powell, V. Rezhets, M. Balogh, and R. Waldo: *Magnesium Technology*, 2001, pp. 175-182.

32. J. Berkmortel, H. Hu, J.E. Kearns, and J.E. Allison: *SAE paper 2000-01-1119*, 2000.

33. M. Pekguleryuz and E. Baril: *Magnesium Technology*, 2001, pp. 119-126.

34. K.Y. Sohn, J.W. Jones, J. Berkmortel, H. Hu, and J.E. Allison: *SAE paper 2000-01-1120*, 2000.

35. M. Pekguleryuz and J. Renaud: *Magnesium Technology*, 2000, pp. 279-284.

36. K.Y. Sohn, J.W. Jones, and J.E. Allison: *Magnesium Technology*, 2000, pp. 271-278.

37. A. Luo and T. Shinoda: *SAE paper 980086*, 1998.

38. A. Luo and B. Powell: *Magnesium Technology*, 2001, pp. 137-144.

39. A. Luo, M. Balogh, and B. Powell: *SAE paper 2001-01-0423*, 2001.

40. B. Powell, A. Luo, V. Rezhets, J. Bommarito, and B. Tiwari: *SAE paper 2001-01-0422*, 2001.

41. M. Suzuki, J. Koike, K. Maruyama, T. Tsudeda, K. Saito, and H. Kubo: *Magnesium Alloys and their Applications*, 2000, pp. 699-704.

42. S. Koike, K. Washizu, S. Tanaka, T. Baba, and K. Kikawa: *SAE paper 2000-01-1117*, 2000.

43. P. Lyon, J.F. King, and K. Nuttall: *Proc. of the 3rd Int. Magnesium Conf.*, 1996, pp. 99-108.

44. L.Y. Wei, G.L. Dunlop, and H. Westengen: *Journal of Materials Science*, 1997, vol. 32, pp. 3335-3340.

45. A. Murphy and R. Payne: *J. Inst. Met.*, 1947, vol. 73, p. 105.

46. I. Polmear: *Light Alloys*, 1989

47. I.P. Moreno, K.Y. Sohn, J.W. Jones, and J.E. Allison: *SAE paper 2001-01-0425*, 2001.

48. C.J. Bettles and M.S. Dargusch: *Magnesium Alloys and their Applications*, 2000, pp. 705-710.

49. K.Y. Sohn, J.W. Jones, and J.E. Allison: University of Michigan, Ann Arbor, MI, unpublished research, 1999.

50. I.P. Moreno, T. Nandy, J.W. Jones, T.M. Pollock, and J.E. Allison: *Scripta Materialia*, 2001, not yet published.

51. F.C. Chen, J.W. Jones, and J.E. Allison: University of Michigan, Ann Arbor, MI, unpublished report, 1996.

52. K.Y. Sohn, J.W. Jones, and J.E. Allison: University of Michigan, Ann Arbor, MI, unpublished research, 2000.

53. X. Su, K.Y. Sohn, D. Dewhirst, and J.E. Allison: *SAE paper 2000-01-1121*, 2000.

54. C.S. Roberts: *Trans AIME*, 1953, vol. 197, p. 1121.

55. C.S. Roberts: *Journal of Metals*, 1956, vol. 6, p. 146-148.

56. L.Y. Wei and G.L. Dunlop: *Magnesium Alloys and their Applications*, 1992, pp. 335-342.

57. G.L. Dunlop and L.Y. Wei: *Proc. 47th Annual World of Magnesium Conf.*, 1990, pp. 61-66.

58. L.Y. Wei, G.L. Dunlop, and H. Westengen: *Metallurgical and Materials Transactions A*, 1995, vol. 26A, pp. 1705-1716.

59. E. Aghion and B. Brontin: *Magnesium Alloys and their Applications*, 1998, pp. 295-300.

60. T.K. Aune, H. Westengen, and T. Ruden: *SAE paper 940777*, 1994.

61. G. Schindelbacher: *Magnesium Alloys and their Applications*, 1998, pp. 247-252.

62. B. Watzinger, P. Wedinger, F. Breutinger, and W. Blum *et al.*: *Magnesium Alloys and their Applications*, 1998, pp. 259-264.

63. B.L. Mordike and P. Lukac: *Proc. of the 3rd Int. Magnesium Conf.*, 1996, pp. 419-424.

64. S.S. Vagarali and T.G. Langdon: *Acta Metallurgica*, 1981, vol. 29, pp. 1969-1982.

65. W. Tegart: *Acta Metallurgica*, 1961, vol. 9, pp. 614-616.

66. I.G. Crossland and R.B. Jones: *Metal Science Journal*, 1972, vol. 6, pp. 162-166.

67. J.E. Morgan and B.L. Mordike: *Strength of Metals and Alloys, 1983, vol. 2, pp. 643-648.*

68. J.E. Morgan and B.L. Mordike: *Metallurgical Transactions A*, 1981, vol. 12A, pp. 1581-1585.

69. W. Henning and B.L. Mordike: *Proc. of the 7th Int. Conf. on the Strength of Metals and Alloys*, 1985, vol. 1, pp. 803-808.

List of Tables and Figures

Table I. Chemical composition of HPDC Magnesium alloys

Alloys	Actual Composition (wt%)								
	Al	Zn	Mn	Si	Fe	Cu	Ni	RE total**	Mg
MEZ	-	0.33	0.26	-	0.01	0.003	<0.001	1.92	Bal.
AE42	3.7	0.005	0.21	-	<0.005	0.003	0.005	2.69	Bal.
AZ91D	8.9	0.72	0.21	0.01	<0.005	0.004	<0.005	-	Bal.

** Rare earth (RE) consists of about 53%Ce, 25%La, 17%Nd, and 5%Pr.

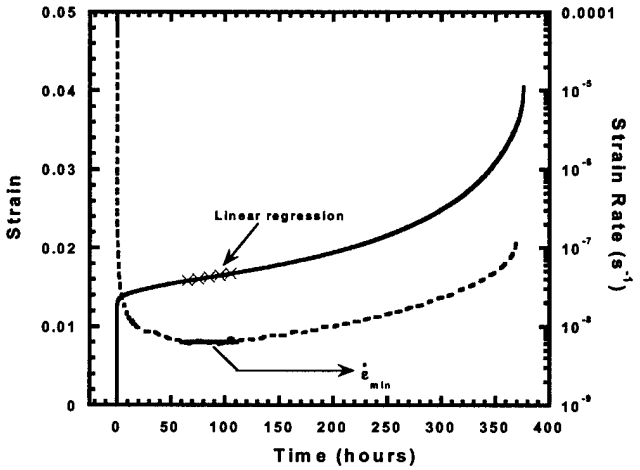

Figure 1. Determination of minimum (steady state) creep rate

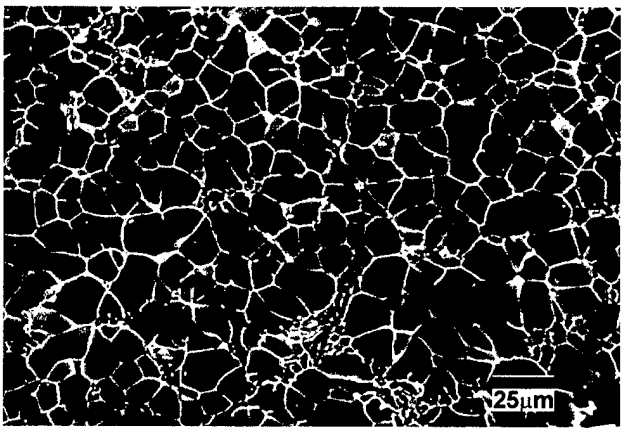

(*a*)

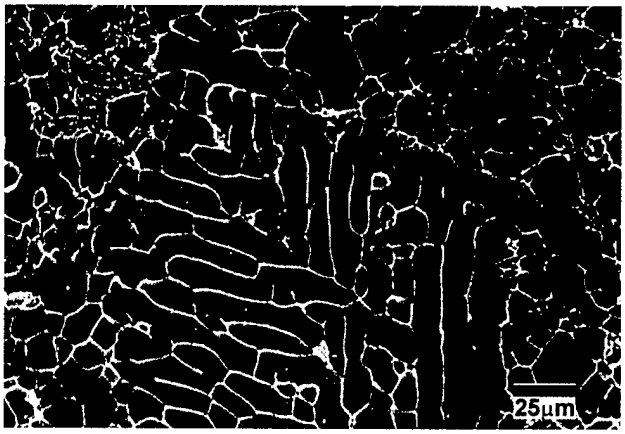

(*b*)

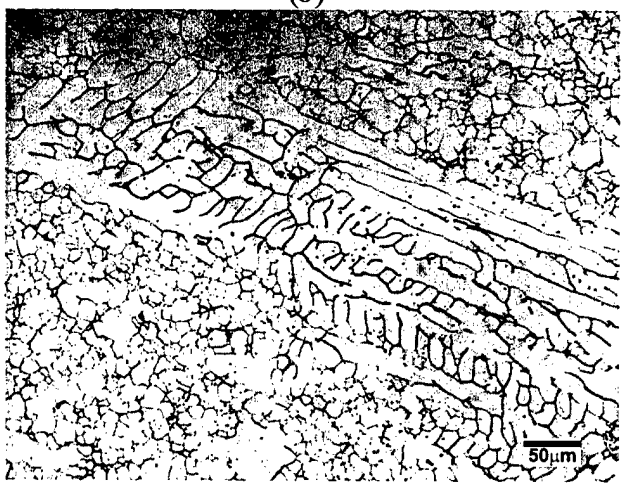

(*c*)

Figure 2. SEM micrographs of the as-cast microstructure of MEZ showing generally (*a*) an equiaxed granular structure and (*b*) occasional patches of cells with higher aspect ratios. A rare existence of more fully developed dendrites are found as shown in the optical micrograph in (*c*).

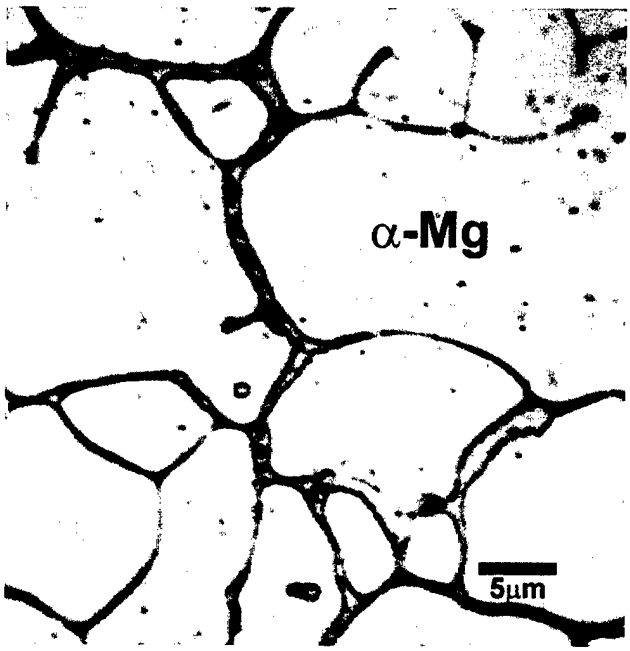

(*a*)

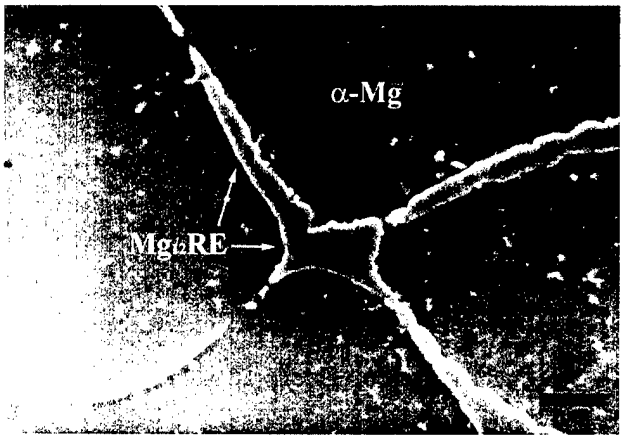

(*b*)

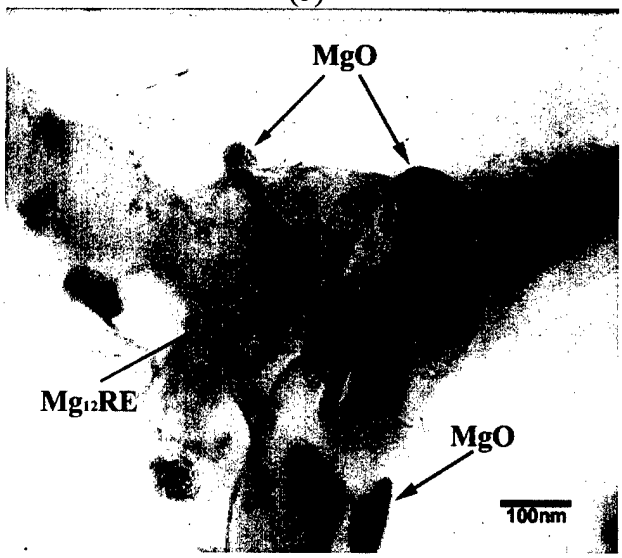

(*c*)

Figure 3. (*a*) Optical, (*b*) SEM SE, and (*c*) TEM BF micrographs of the grain boundary region in as-cast MEZ. Dark spots within α-Mg dendrites of (*a*) are pitting defects resulting from etching

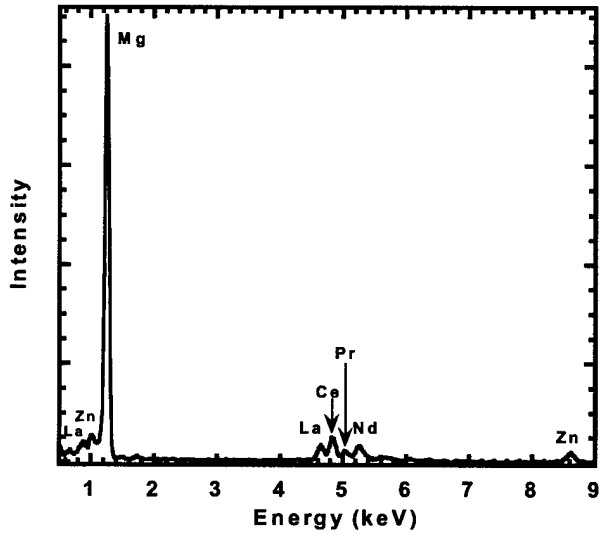

(*a*)

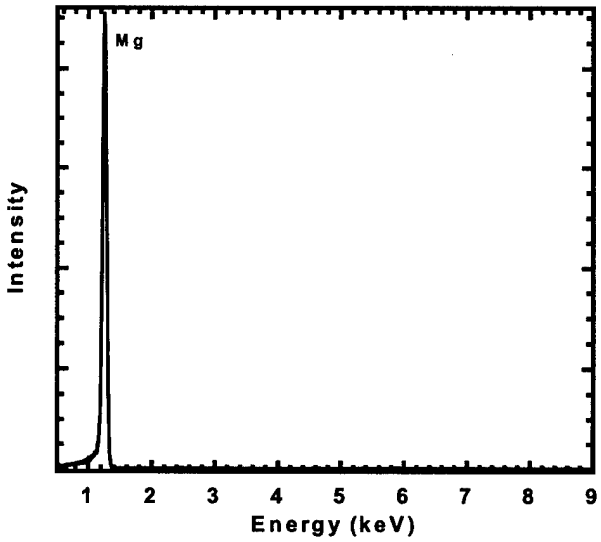

(*b*)

Figure 4. TEM/EDS spectra of MEZ's (*a*) grain boundary phase and (*b*) matrix phase

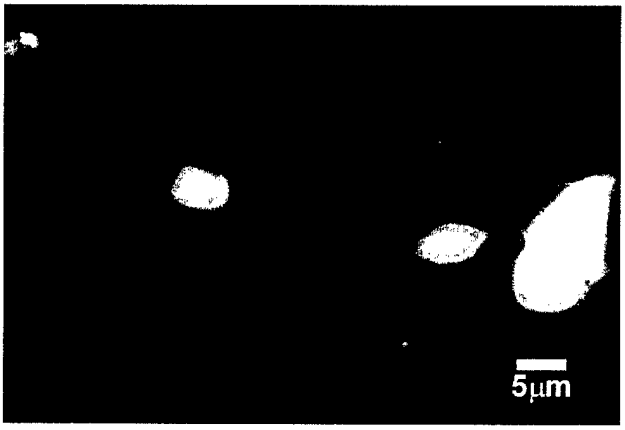

Figure 5. Back-scattered electron SEM micrograph of MEZ, thermally exposed at 590°C for 25.5 hours and naturally cooled

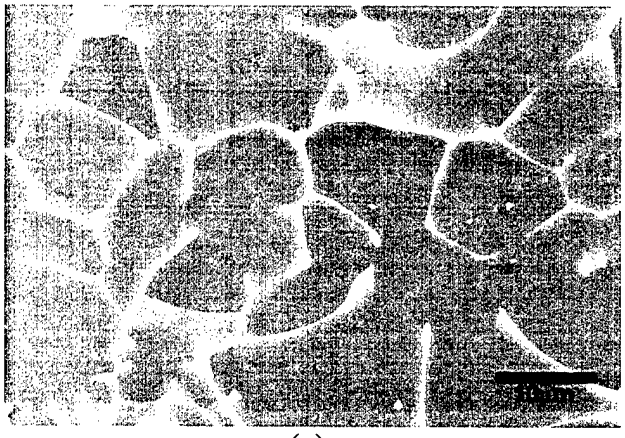

(*a*)

(*b*)

Figure 6. SEM micrograph of MEZ (*a*) as cast and (*b*) crept at 175°C, 60MPa

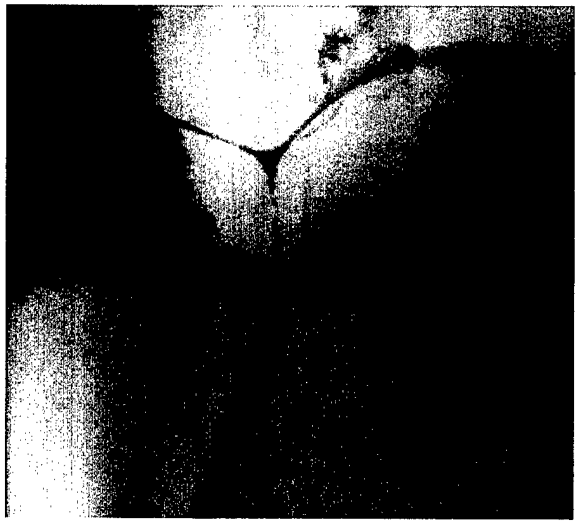

(*a*)

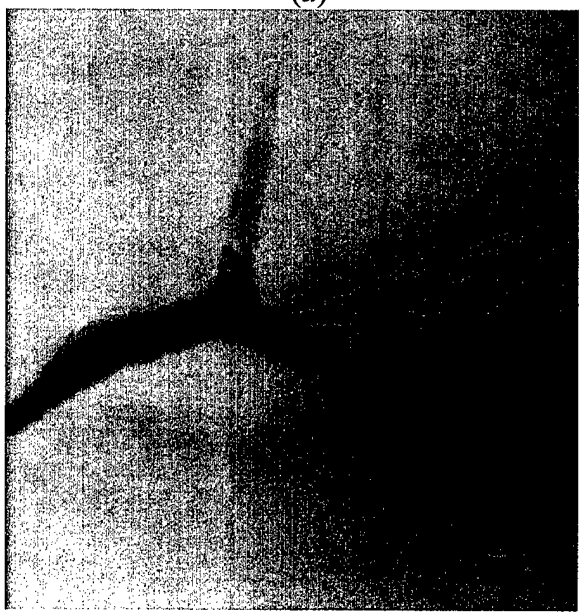

(*b*)

Figure 7. TEM micrographs of grain boundary region of MEZ (*a*) as-cast and (*b*) crept at 150°C, 80MPa.

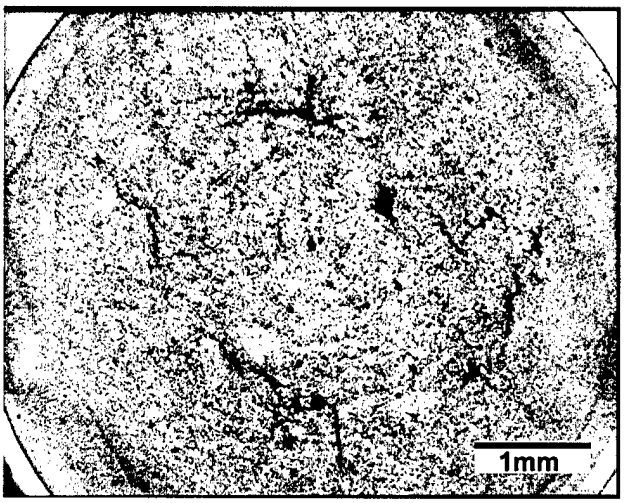

(*a*)

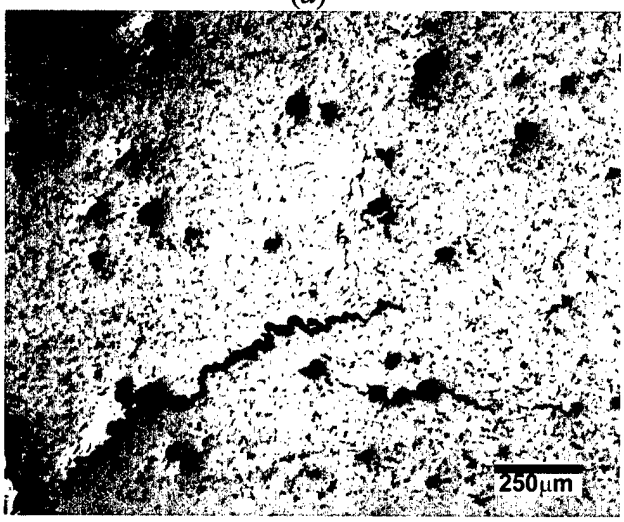

(*b*)

Figure 8. Optical micrographs showing porosity/intergranular cracks in the gage section of as-cast MEZ

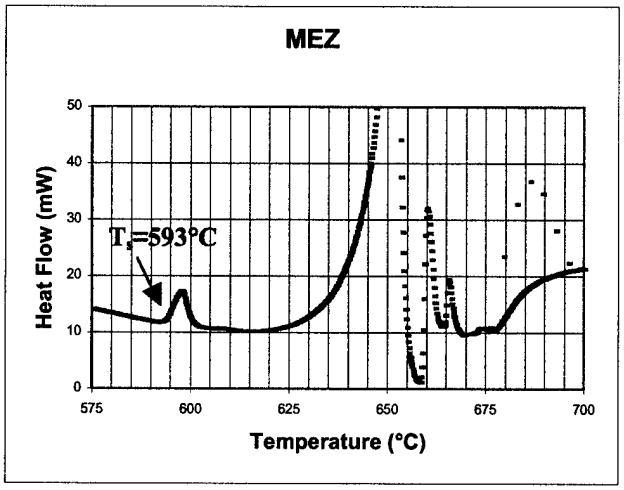

Figure 9. Solidus temperature, T_s, of MEZ determined by differential scanning calorimetry

Table II. Homologous temperature values for die cast alloys. AE42 and AZ91D data were obtained from previous work[49]

	MEZ	AE42	AZ91D
T_s	593°C	613°C	480°C
125°C	0.46	0.45	0.53
150°C	0.49	0.48	0.56
175°C	0.52	0.51	0.59

Table III. Mechanical properties of die cast MEZ

Temp. (°C)	YS (MPa)	UTS (MPa)	Elong. (%)
RT	97.6	134.8	2.9
125	83.6	115.9	6.8
150	78.0	110.0	7.5
175	73.5	99.7	5.0

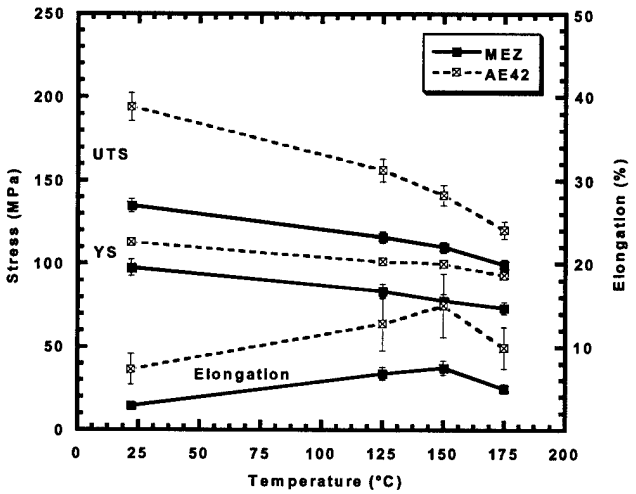

Figure 10. Mechanical properties of die cast MEZ and AE42 at various temperatures. (AE42-175°C data from previous work[49] obtained by crosshead displacement measurement)

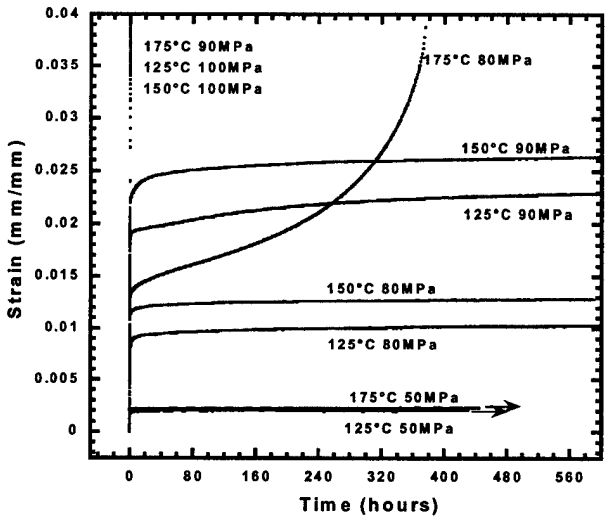

Figure 11. Tensile creep behavior of MEZ at various temperatures and initial stresses

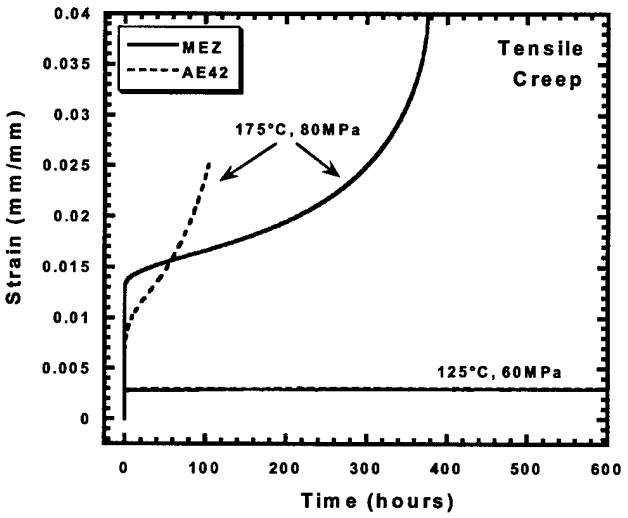

Figure 12. Comparison of the tensile creep behavior of MEZ and AE42

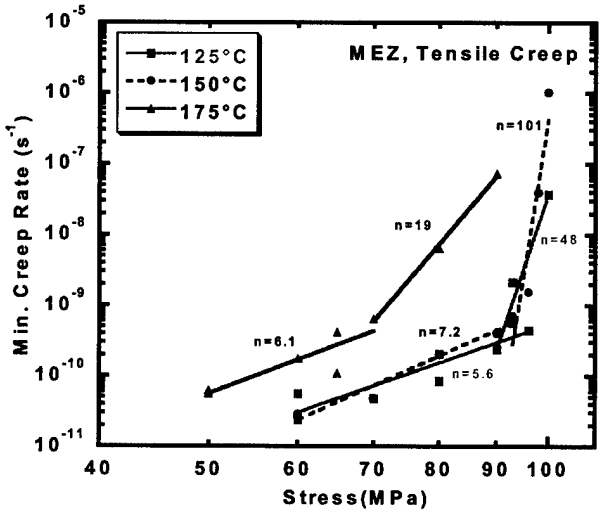

Figure 13. Effect of stress on the minimum creep rate of MEZ

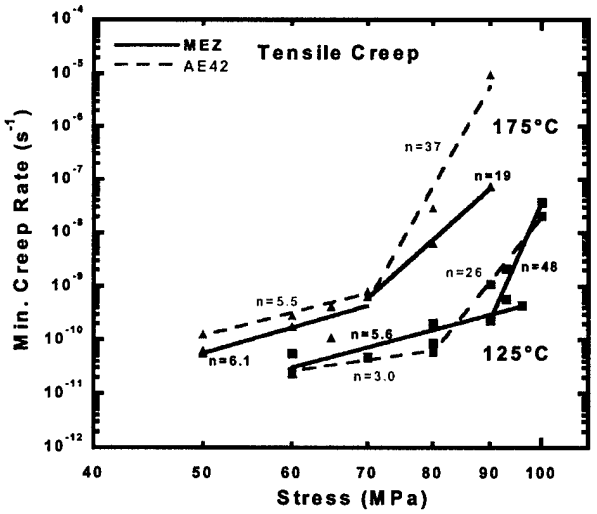

Figure 14. $\dot{\varepsilon}_{min}$ dependency on stress – a comparison between MEZ and AE42

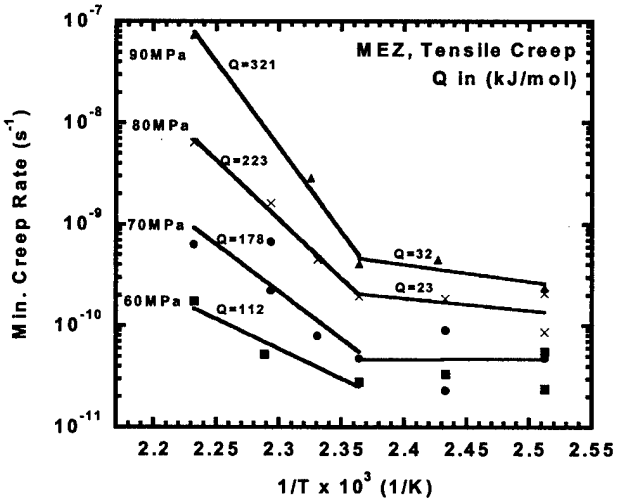

Figure 15. Effect of temperature on the minimum creep rate of MEZ

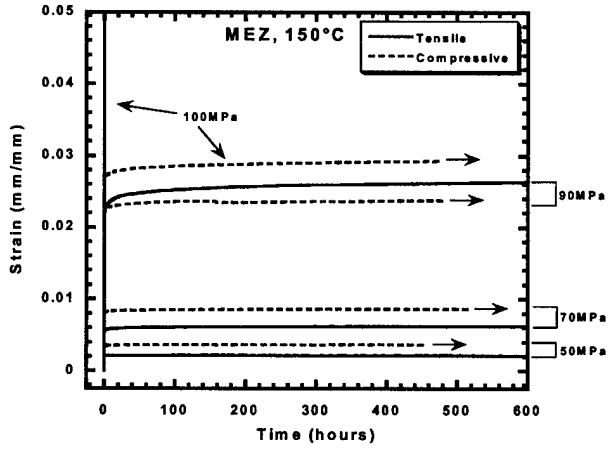

Figure 16. Comparison of the tensile and compressive creep behavior of MEZ

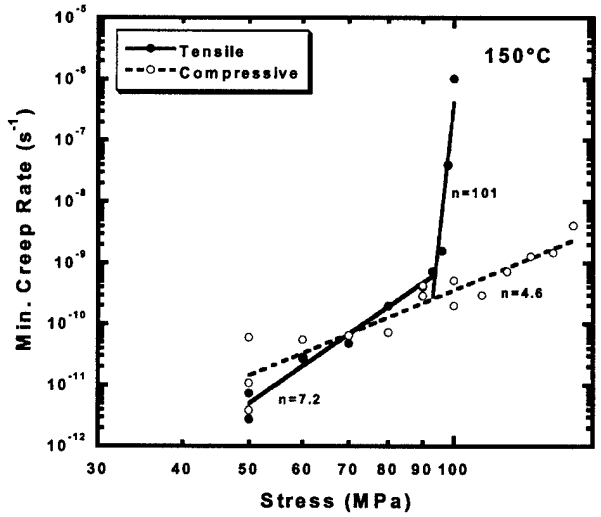

Figure 17. Comparison of the tensile and compressive $\dot{\varepsilon}_{min}$ dependency on stress

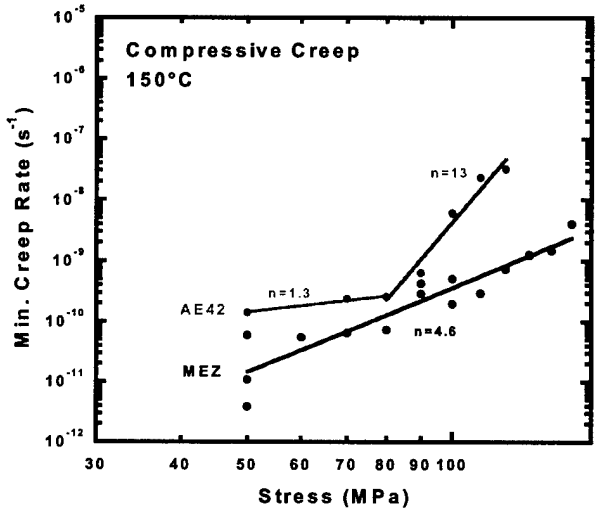

Figure 18. $\dot{\varepsilon}_{min}$ dependency on stress – a comparison between MEZ and AE42

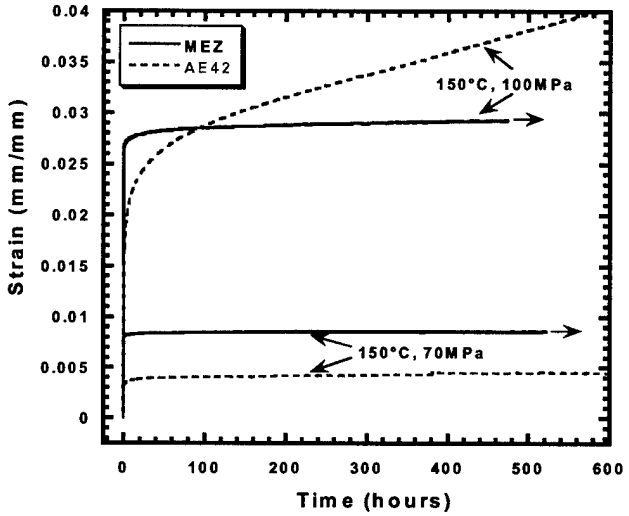

Figure 19. Comparison of the compressive creep behavior of MEZ and AE42

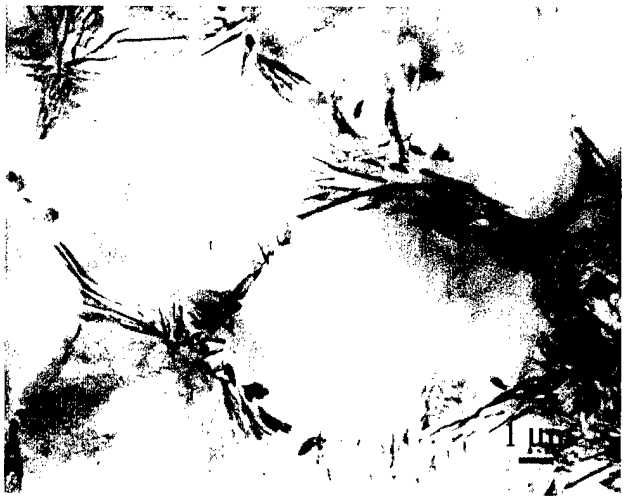

(*a*)

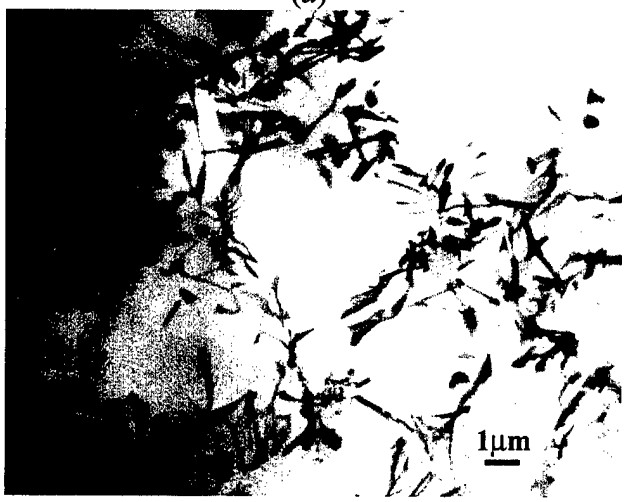

(*b*)

Figure 20. TEM micrographs of AE42 (*a*) as cast and (*b*) crept at 150°C, 85MPa (work done previously[52])

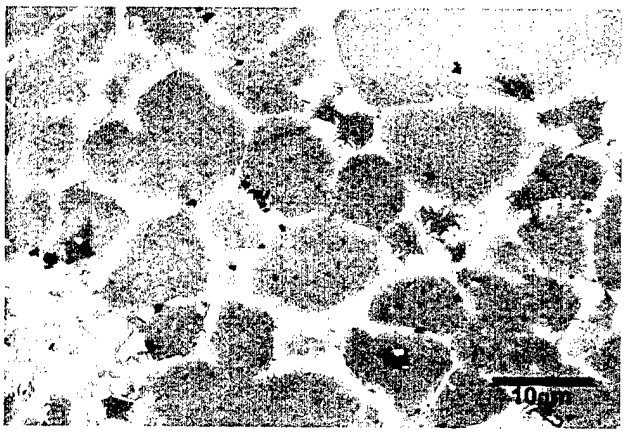

(*a*)

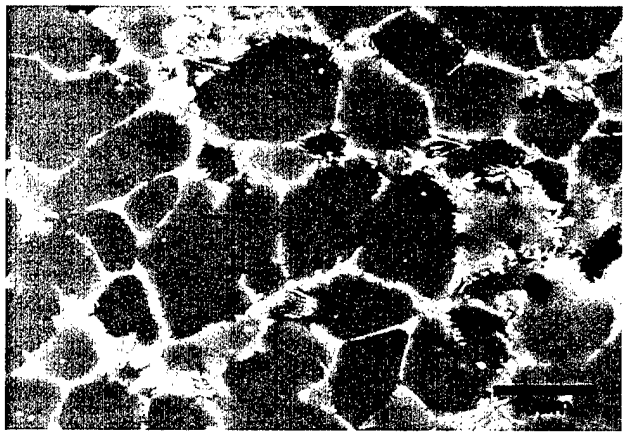

(*b*)

Figure 21. SEM micrograph of AE42 (*a*) as cast and (*b*) crept at 175°C, 70MPa

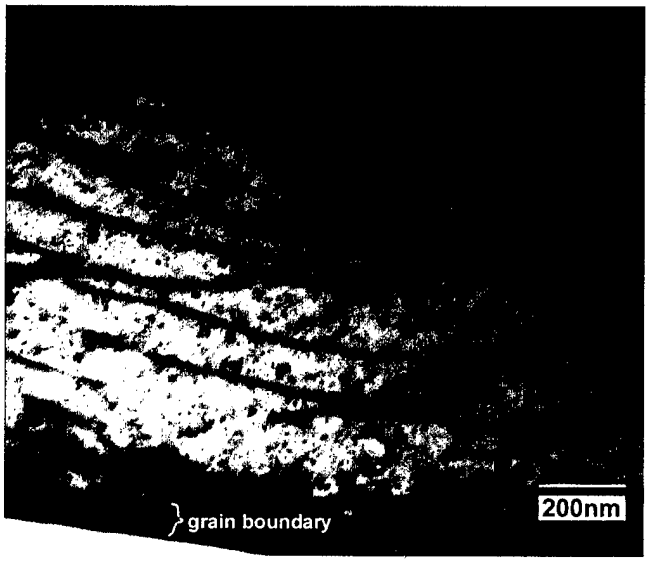

Figure 22. Dislocation substructure of MEZ after 350 hours of steady-state creep (150°C, 80MPa) near $[10\bar{1}\,1]$ zone axis ($g=\bar{1}011$)